Solar Adoption as Agricultural Adaptation: Evidence from California's Central Valley*

Cam McClure† Erik Katovich‡

March 5, 2026

Abstract

Does expansion of utility-scale solar energy threaten agricultural communities or offer them an economic lifeline? Using a parcel-level dataset spanning 2006-2023, we assess drivers of utility-scale solar adoption in California's Central Valley – one of the United States' most critical agricultural regions. We find that solar adoption concentrates on parcels where agricultural viability is low and solar potential is high: specifically, drought-exposed lands with poor soil, high farm labor costs, low-value crops, large parcel size, proximity to electricity transmission infrastructure, and strong solar irradiance. Results align with a conceptual framework in which landholders choose agriculture or solar leasing to maximize expected returns from their land. We identify optimal sites that could generate 25.2 GW of solar energy, or 44% of California's 2045 target, on marginal non-urban land parcels in the Central Valley.

Keywords: Solar Energy, Climate Adaptation, Agriculture, Land Use, Drought
JEL Codes: Q15, Q42, R14, Q54, Q24

*Acknowledgments: We thank Dan Wanyama for guidance on constructing the drought severity index.
†Department of Agricultural and Resource Economics, University of Connecticut
‡Corresponding Author. Department of Agricultural and Resource Economics, University of Connecticut: erik.katovich@uconn.edu

1 Introduction

The global transition to renewable energy is accelerating, with renewable energy capacity forecast to grow by 2-3 times between 2024 and 2030 (IEA, 2024). Among electricity generation options, utility-scale solar stands out due to its low levelized cost of energy (Lazard, 2025). Despite this cost advantage and contributions to reducing carbon emissions and air pollution (Rivera et al., 2024), utility-scale solar raises concerns over the amount and type of land it replaces, with particular concern over displacement of farmland and trade-offs between clean energy and food production (Stid et al., 2025; Battersby, 2023; Moore et al., 2022; Hernandez et al., 2015).

This study focuses on California's Central Valley, an ideal location to examine trade-offs between agricultural land-use and solar energy development (Stid et al., 2022). The Central Valley supplies approximately 40% of the United States' fruits, nuts, and vegetables and accounts for 8% of total U.S. agricultural output despite occupying just 1% of U.S. farmland (USGS, 2023). However, characteristics that make the Central Valley an ideal location for agriculture, such as abundant sunlight, relatively flat land, and proximity to major population centers, also make it an ideal location for utility-scale solar projects. The number of these projects operating in the Central Valley increased from 0 in 2006 to 215 in 2023, with an average size of 52 hectares per project. Moreover, the Central Valley has experienced accelerating groundwater depletion since 2003 (Liu et al., 2022), jeopardizing agricultural viability and presenting utility-scale solar as a potential adaptation strategy for landholders.

Understanding which parcels convert to solar and why landholders make this choice is essential for managing tradeoffs between clean energy expansion and food production. From the landholder's perspective, solar adoption represents a forward-looking decision that weighs solar lease payments against uncertain agricultural returns shaped by drought risk, farm labor costs, and soil suitability for agriculture. Comprehensive empirical evidence on how these factors influence adoption decisions is limited, leaving policymakers without clear guidance on where solar development is likely to occur and which agricultural lands are most vulnerable to conversion.

To analyze property-level determinants of utility-scale solar adoption, we construct a novel panel dataset encompassing the universe of non-urban land parcels in California's Cen-

tral Valley between 2006-2023.[1] For each parcel, we observe parcel size, solar radiation intensity, distance to electricity transmission infrastructure, and soil suitability for agriculture (a measure that incorporates soil depth, surface texture, subsoil characteristics, and groundwater quality), as well as annual land use, agricultural labor costs, drought exposure, and the spatial footprint of utility-scale solar energy installations. Using these granular data, we estimate the influence of parcel characteristics on landholders' solar adoption decisions at both the extensive margin (solar = 0/1) and intensive margin (square meters installed). Our baseline specification includes both time-varying factors (i.e., lagged drought exposure and labor costs) and time-invariant parcel characteristics. We also estimate models with parcel fixed effects, where we estimate interactions between time-invariant characteristics and drought exposure to measure heterogeneity in drought responsiveness. Finally, we identify land use classes replaced by solar installations to quantify how much high-value farmland is being lost and assess which land uses are most likely to switch to solar.

Descriptive results reveal systematic patterns in solar siting. Solar facilities concentrate in areas with higher drought exposure, stronger solar irradiance, and closer proximity to electrical substations compared to the overall parcel distribution. Solar siting is more dispersed across the agricultural suitability distribution: 69% of installations are on parcels in the bottom half of the suitability distribution, 24% are on parcels in the top two quintiles, representing prime agricultural land. Nevertheless, solar facilities are underrepresented in the highest-suitability deciles relative to the overall parcel distribution.

Between 2006 and 2023, cereal grains and fallow/idle cropland were the land types most often converted to solar, with 4,146ha (0.59% of total cereal grain area) and 3,836ha (0.78% of total fallow or idle cropland) converted, respectively. High-value permanent crops such as fruits and nuts experienced substantially lower conversion rates, consistent with landowners preserving sunk investments in perennial plantings. In total, approximately 10,800 hectares in the Central Valley were converted to utility-scale solar during this period, representing 0.23% of the region's non-urban land area.

Regression results reveal that utility-scale solar adoption increases significantly with drought exposure, local agricultural labor costs, parcel size, solar irradiance, proximity to electrical

[1] We observe 244,878 property boundaries for non-urban parcels. We exclude urban parcels because no utility-scale solar facilities were constructed in these areas during the study period.

substations, and poor soil quality. Standardized coefficients indicate that parcel size, drought, and grid access are the strongest predictors, followed by solar irradiance, labor costs, and soil quality. Regressions including prior-period land use confirm that parcels with fallow/idle cropland, developed land (e.g., developed open space), barren shrubland, and cereal grains are more likely to convert to solar relative to grassland/pasture, while high-value crops like nuts, fruits, and vegetables are less likely to convert. Adoption likelihood also rises in the number of years cropland has been fallow or idle. Interaction analysis reveals that the marginal effects of both drought and local agricultural labor costs increase with parcel size, solar irradiance, proximity to electrical substation, and poor soil quality, indicating that solar adoption decisions are multi-dimensional and respond to multiplicative effects across drivers.

Finally, we construct a suitability index to identify non-solar parcels that are both technically attractive for solar development and economically marginal for agriculture. Using penalty functions that reward proximity to transmission infrastructure, large parcel size, high drought exposure, strong solar irradiance, poor soil quality, and low-value land uses, we identify 328 high-suitability sites (0.1% of total non-urban parcels) that could generate 25.2 GW of utility-scale solar energy, representing 44% of California's 2045 renewable energy target. These optimal sites would concentrate solar development on marginal agricultural lands while meeting a substantial share of the state's clean energy goals, demonstrating that renewable energy expansion and agricultural preservation are not in fundamental conflict. We validate the predictive power of our index by calibrating it on 2006-2018 data and predicting post-2018 adoption, finding that 87% of post-2018 parcels are installed in the top 3 deciles of predicted suitability.

To rationalize our results, we develop a conceptual framework in which a forward-looking parcel holder chooses whether to (i) continue with agriculture or (ii) allow a solar developer to lease their parcel to maximize expected returns from their land, accounting for their parcel's unique characteristics and Bayesian updating based on prior drought exposure and labor costs. Together, our parcel-level empirical analysis and conceptual framework demonstrate that solar expansion in the Central Valley is not the result of random farmland displacement, but rather a systematic response by landholders to agricultural viability, solar economics, and infrastructure access.

1.1 Related Literature and Contributions

The rapid expansion of utility-scale solar energy generation has prompted a growing body of research on determinants of solar adoption and the environmental trade-offs and impacts of these facilities. We contribute to three strands of this literature: (i) geospatial and economic drivers of solar siting, (ii) interactions between utility-scale solar and agriculture, and (iii) landholder adaptation to climate shocks. We advance each of these literatures through a data-rich, parcel-level, longitudinal analysis of solar adoption decisions in one of the world's most important agricultural regions.

Prior studies have identified physical and economic factors shaping the location of utility-scale solar development. Solar adoption is highest in areas with abundant solar radiation, low humidity, and moderate temperatures (Adeh et al., 2019), which often corresponds to croplands and grasslands. Furthermore, solar development has been found to disproportionately replace cultivated cropland, rather than brownfields or natural land cover – likely due to lower site preparation costs (Evans et al., 2023; Hernandez et al., 2015). Proximity to electricity transmission infrastructure is critical for economic feasibility, as interconnection costs can exceed $1 million per project if new transmission lines are required (Lease, 2022). Institutional incentives also drive expansion. For instance, California's Renewable Portfolio Standard (RPS) and SB 100 mandate 100% renewable electricity by 2045 (CEC, 2021a,b). As land competition intensifies, solar developers increasingly seek to optimize energy density and minimize land costs, leading them to prioritize larger parcels (Bolinger and Bolinger, 2022; Daniels and Wagner, 2022). Our analysis leverages exceptionally detailed parcel-level geospatial data to quantify and compare the relative magnitude of these factors during a period of major solar expansion (2006-2023).

Another body of literature examines trade-offs between solar development and agriculture. Some farmers view solar leasing as a temporary land use that supports long-term agricultural viability, likening it to a 25-30 year "cover crop" (Goldberg, 2023). "Agrivoltaics" offers a mixed land use strategy by co-locating solar and agriculture or livestock, though commercial viability remains limited (Daniels, 2023; Pascaris et al., 2021). Solar may also provide environmental co-benefits, such as water savings relative to irrigated cropland (Stid et al., 2022), making "solar fallowing" a potential drought adaptation strategy (Buckley Biggs et al.,

2022). Policymakers have sought to steer solar development toward impaired or marginal lands (Hoffacker et al., 2017; Plan, 2025; Kaenel and Venteicher, 2024), though most adoption decisions are still driven by individual landholder incentives. We contribute to this literature by quantifying which crop types and land uses are most likely to be replaced by solar in the Central Valley. We further contribute by introducing a simple but informative conceptual framework to explain landholders' decision-making between agriculture and solar.

Finally, there is a growing literature focused on how landowners adapt to climate shocks, including drought. Chandanpurkar et al. (2025) document continental drying and mega-drought regions across the Northern Hemisphere, and Liu et al. (2022) document accelerating groundwater depletion in California's Central Valley. In response, farmers in the Central Valley have shifted toward higher-value perennial crops while reducing lower-value annual crops (Mount and Hanak, 2019; Alvar Escriva-Bou and Viers, 2022; Ellen Hanak and MacEwan, 2017; Carman, 2019). Water scarcity has also driven crop switching and land fallowing (Medellín-Azuara et al., 2012; Wartenberg et al., 2021). Wealthier landowners are better positioned to adapt to drought, creating unequal distributional effects (Visser et al., 2024). Our analysis extends this literature by measuring how drought exposure interacts with parcel characteristics to shape solar adoption as an adaptation strategy in the face of changing environmental conditions.

2 Conceptual Framework

Suppose that parcel owners face a forward-looking land use decision: whether to continue using their land for agriculture or lease it to a solar energy developer. If solar panels are installed, the land is removed from agricultural production and generates a stream of lease payments for approximately 25 years. From the parcel owner's perspective, this choice involves comparing the net present value (NPV) of two mutually exclusive options:[2]

- **Agricultural use**, which yields uncertain long-term profits depending on evolving mar-

[2]Agrivoltaics, or the co-location of agriculture and solar panels, allows landholders to combine agricultural production with solar energy generation rather than treating them as mutually exclusive uses. In practice, this can involve grazing sheep to manage vegetation under and around panel arrays, or cultivating low-growing, shade-tolerant crops such as lettuce, strawberries, or peppers beneath elevated panels. Despite their potential to reduce land use tradeoffs, agrivoltaic systems have yet to gain traction in California's Central Valley, with only 2 of the 215 cited solar facilities currently reporting multiple land uses as of 2023.

ket prices and drought conditions

- **Solar leasing**, which guarantees fixed, inflation-adjusted payments over a 20 to 30-year horizon with no labor or input costs.

Let $D_i \in \{A, S\}$ denote the land use choice for parcel i, where A represents agriculture and S solar leasing, and let T denote the duration of a typical solar lease.

2.1 Agricultural Returns

Let $\mathbb{E}[\pi_{it}^A]$ denote the landholder's expected annual net return from agriculture on parcel i in future period $t + \tau$. Expected agricultural returns depend on parcel characteristics, current land use, and beliefs about future drought exposure and agricultural labor costs:

$$\mathbb{E}_t[\pi_{i,t+\tau}^A] = f(\text{Suitability}_i,\ \text{CurrentUse}_{it},\ \mathbb{E}_t[d_{i,t+\tau}],\ \mathbb{E}_t[w_{i,t+\tau}]) \tag{1}$$

where d_{it} denotes drought exposure and w_{it} denotes farm labor costs. Function $f(\cdot)$ is hypothesized to be increasing in *agricultural suitability*, dependent on *current land use* (because parcels with pasture or temporary crops may be more likely to adopt solar than those with permanent crops), and decreasing in *expected drought exposure* and *expected farm labor costs*.

Bayesian Learning We assume landholders form expectations about d_{it} and w_{it} through Bayesian updating based on recent observed conditions. Specifically, suppose realized drought exposure and labor costs can be decomposed into an unknown parcel-specific mean component and transitory shocks:

$$d_{it} = \mu_{di} + \varepsilon_{it}^d \qquad w_{it} = \mu_{wi} + \varepsilon_{it}^w \tag{2}$$

where μ_{di} and μ_{wi} are unknown long-run mean conditions for parcel i, and ε_{it}^d and ε_{it}^w are mean-zero shocks. At time t, the landholder observes $(d_{i,t-1}, w_{i,t-1})$ and updates beliefs about (μ_{di}, μ_{wi}). Under conjugate priors, the posterior mean is a convex combination of the prior mean m and the most recent realization:

$$\mathbb{E}_t[\mu_{di}] = (1 - \omega_d)m_{d0} + \omega_d d_{i,t-1} \qquad \mathbb{E}_t[\mu_{wi}] = (1 - \omega_w)m_{w0} + \omega_w w_{i,t-1} \tag{3}$$

for weights $\omega_d, \omega_w \in (0, 1)$ that summarize the relative precision of prior beliefs and the informativeness of observed conditions. We assume expectations of future drought exposure

and labor costs are anchored by these posterior means, implying that higher recent drought exposure or labor costs increase expected future exposure and costs, lowering expected agricultural returns through function $f(\cdot)$ in Equation (1).

Agricultural net present value. Under the simplifying assumption that agricultural land retains productive value over time,[3] we define the time-t present value of continuing in agriculture over the duration T of a typical solar lease, given discount factor $\delta \in (0, 1)$, as:

$$\mathbb{E}_t[V_{it}^A] = \sum_{\tau=0}^{T-1} \delta^\tau \, \mathbb{E}_t[\pi_{i,t+\tau}^A]. \tag{4}$$

In our empirical analysis, lagged drought exposure and labor costs on parcel i in the previous three years proxy for the information used to form $\mathbb{E}_t[d_{i,t+\tau}]$ and $\mathbb{E}_t[w_{i,t+\tau}]$.

2.2 Solar Leasing Returns

Let R_{i0}^S be the initial lease payment offered by a solar developer for parcel i. Contracts typically include an annual escalation factor γ (e.g., 2% per year) to adjust for inflation. The total lease payment in year t is:

$$R_{it}^S = R_{i0}^S \cdot (1+\gamma)^t$$

The NPV of a T-year solar lease is:

$$V_i^S = R_{i0}^S \cdot \sum_{t=0}^{T-1} [\delta(1+\gamma)]^t = R_{i0}^S \cdot \frac{1-\theta^T}{1-\theta} \quad \text{where } \theta = \delta(1+\gamma) < 1$$

The lease rate R_{i0}^S depends on:

$$R_{i0}^S = g(\text{SolarRadiation}_i, \text{GridDistance}_i, \text{Size}_i)$$

This function is hypothesized to be increasing in *solar irradiation*, decreasing in *distance from electricity grid infrastructure*, and increasing in *parcel size*, given that more solar radiation generates more electricity, long-distance grid connections are costly, and larger parcels enable economies of scale in permitting, installation, and operations – increasing solar developers' willingness to pay for these characteristics.

[3] If sustained cultivation depletes soil fertility or groundwater stocks while "solar fallowing" allows regeneration during the lease term, this would provide an additional incentive for solar adoption not captured in the baseline framework.

2.3 Parcel Owner's Decision Rule

Notably, expected returns from agriculture depend on uncertain future outcomes, while returns from solar depend on observable baseline characteristics. A risk-neutral landowner[4] thus chooses the option with higher NPV at time t:

$$D_{it} = \begin{cases} S & \text{if } V_{it}^{S} > \mathbb{E}_t[V_{it}^{A}] \\ A & \text{otherwise,} \end{cases}$$

This framework predicts that landholders are more likely to adopt solar when expected agricultural profits are low (e.g., due to poor soil, high labor costs, or drought exposure), solar potential is high (e.g., due to strong solar radiation or proximity to grid infrastructure), and parcel size is large (enabling cost efficiencies in solar installation and operations). Empirical calibration of each parameter in agricultural and solar return functions $f(\cdot)$ and $g(\cdot)$ is undertaken in the following sections.

3 Data

This section discusses data sources and processing steps to prepare the parcel-level panel dataset (2006-2023) used in empirical analyses.

3.1 Parcels

Parcels serve as the primary unit of analysis. The base parcel boundary layer (as of 2013) is drawn from the California Statewide Parcel Boundaries dataset (LACounty, 2025). Missing counties are supplemented using county-level GIS portals. Parcel data does not report information on owners, limiting our ability to analyze the effects of owner characteristics on solar adoption. To focus the analysis on land where solar development is feasible, we exclude parcels identified as urban in the National Land Cover Dataset (NLCD) as of 2023, given that no utility-scale solar facilities were built in urban areas during the study period. The result-

[4]This risk-neutral framework can be extended to incorporate risk aversion. For a landowner with constant absolute risk aversion parameter $\rho > 0$, the certainty equivalent of perpetual agricultural returns is $CE(V_{it}^{A}) = \frac{1}{1-\delta}\left[\mathbb{E}[\pi_{it}^{A}] - \frac{\rho}{2}\sigma_{itA}^{2}\right]$, where σ_{itA}^{2} is the variance of annual agricultural profits. Risk aversion parameter ρ could vary across landholders based on individual preferences, wealth, access to crop insurance, off-farm employment opportunities, or other risk-hedging mechanisms. Under this framework, parcels with high agricultural profit volatility would face a higher risk premium $\frac{\rho}{2}\sigma_{itA}^{2}$, providing additional motive for solar adoption.

ing parcel boundaries, shown in Figure 1, are intersected with geospatial datasets described in the following sections to construct the parcel-year panel.

Figure 1: Non-Urban Parcels

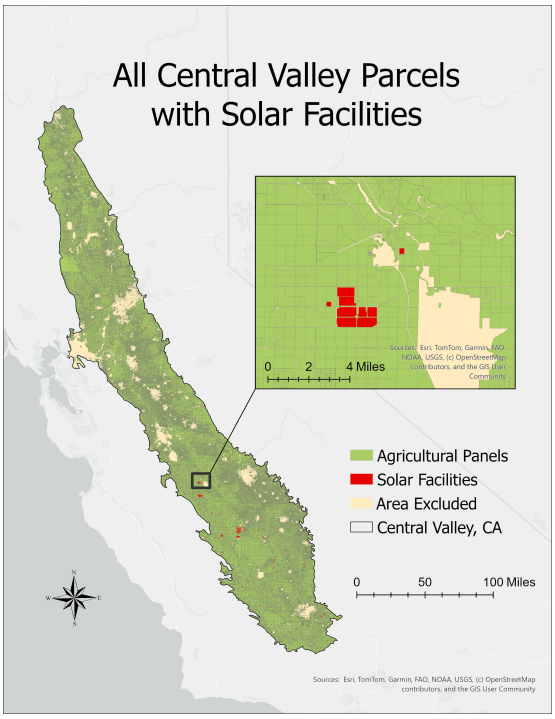

Figure 2: Solar Facilities by Size

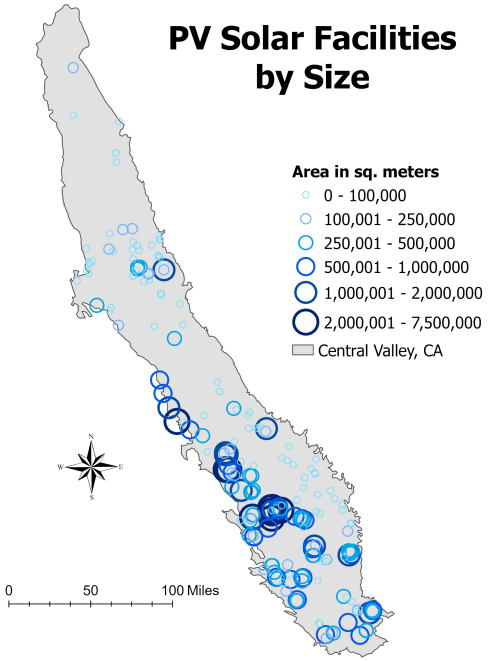

3.2 Solar Facilities

Data on utility-scale solar installations are from the U.S. Solar Photovoltaic Database (Fujita et al., 2023). This dataset includes year of installation, facility size (ancillary infrastructure such as substations or maintenance facilities), and energy capacity for all utility-scale solar facilities with more than 1MW of capacity installed in the United States between 2006-2023. 215 solar facilities are recorded within the study region during this period. Parcels are coded as having a solar facility in year t if any portion of a utility-scale solar site falls within the parcel boundary in that year. Some installations cross parcel boundaries and are thus recorded for multiple parcels. Total solar-covered area is measured in square meters per parcel-year. Figure 2 presents the location and relative size of these facilities.

3.3 Drought

Drought exposure is measured using the U.S. Drought Monitor (USDM) (University of Nebraska–Lincoln, 2025), which provides weekly maps of drought severity across the United States at 500m resolution. The USDM integrates multiple physical indicators, including precipitation, streamflow, reservoir levels, temperature, soil moisture, vegetation health, and expert field assessments. Drought is categorized into five levels: Abnormally Dry (D0), Moderate (D1), Severe (D2), Extreme (D3), and Exceptional (D4). Based on these scores, the Drought Severity and Coverage Index (DSCI) (Akyuz, 2017) constructs a continuous measure of drought severity. DSCI assigns integer weights to each category each week: 1 to D0, 2 to D1, through 5 to D4, yielding a maximum possible annual score of 500. We normalize DSCI scores to a 0–1 scale. Figure 3 presents average annual drought intensity over time, with years of declared historic drought highlighted.

Figure 3: Drought Exposure Over Time

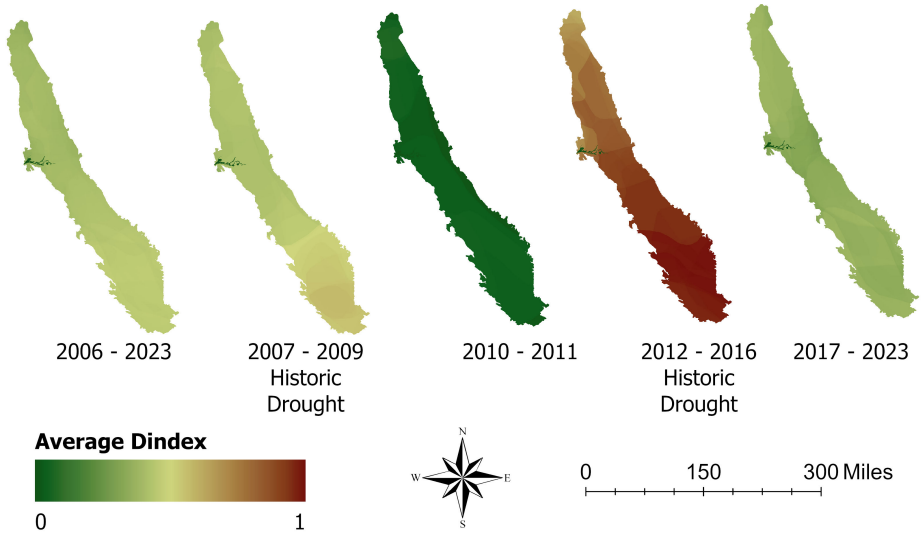

3.4 Crops

Crop coverage for 2007 through 2023 is drawn from the USDA National Agricultural Statistics Service (2023), which provides land cover information at a 30m-by-30m resolution. We re-classify crops into 12 agricultural groups: Cereal Grains; Feed, Fiber, and Industrial Crops; Fruits; Vegetables and Melons; Nuts; Tree Crops; Fallow/Idle Cropland; Grass-

land/Pasture; Water; Developed Land; Barren/Shrubland; and Forest/Wetlands. The breakdown of these categories is listed in Table A1. Figure 4 illustrates the reclassified layer for 2022. Because 2007 is the first year where reliable crop information is recorded for California's Central Valley, installation of a single solar facility in 2006 is omitted from the analysis. We identify the agricultural land use for each parcel-year as the modal crop type in that year, enabling identification of specific crop types displaced by solar development.

Figure 4: Reclassified 2022 CDL Layer

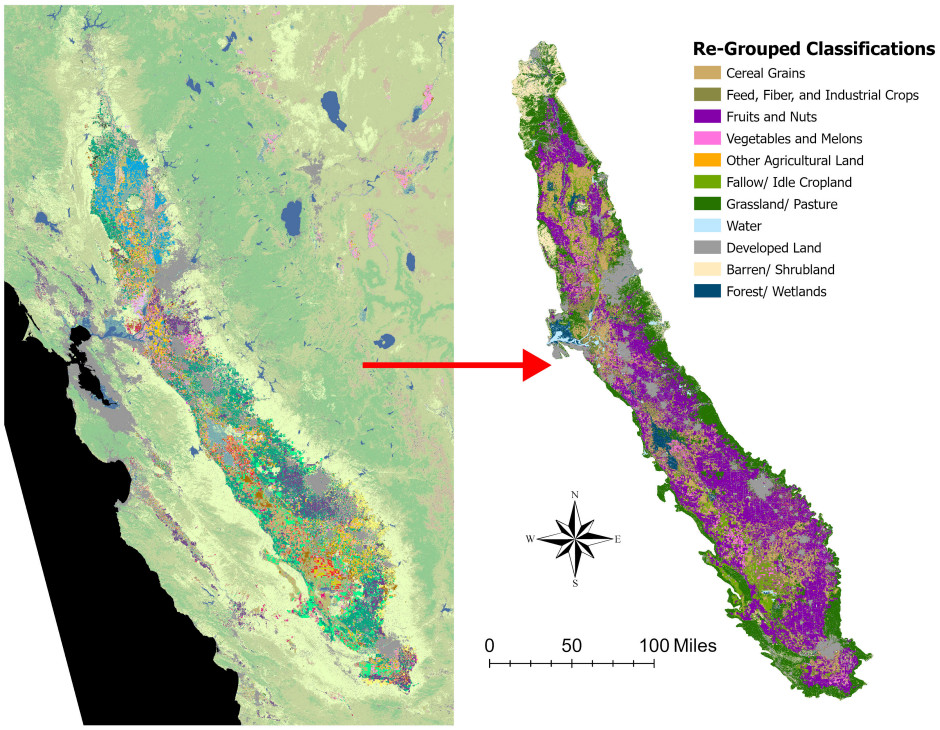

3.5 Agronomic Suitability

Agronomic suitability data are obtained from the Conservation Biology Institute (2024), which processes soil information reported by the Natural Resources Conservation Service (2022) to generate an agricultural potential index. The index incorporates factors such as soil depth, surface texture, subsoil composition, and groundwater quality to estimate agronomic potential, expressed as a percentage. We rescale this percentage to a 0 to 1 range and invert it so that higher values indicate poorer suitability for agriculture. The SSURGO dataset does

not cover the full extent of the Central Valley, resulting in the exclusion of 27 solar facilities. Excluded areas are shown in gray in Figure 5. We estimate a robustness check where we drop the agricultural suitability variable to retain all solar facilities in sample and find that estimates for the remaining covariates are stable.

Figure 5: Agricultural Suitability

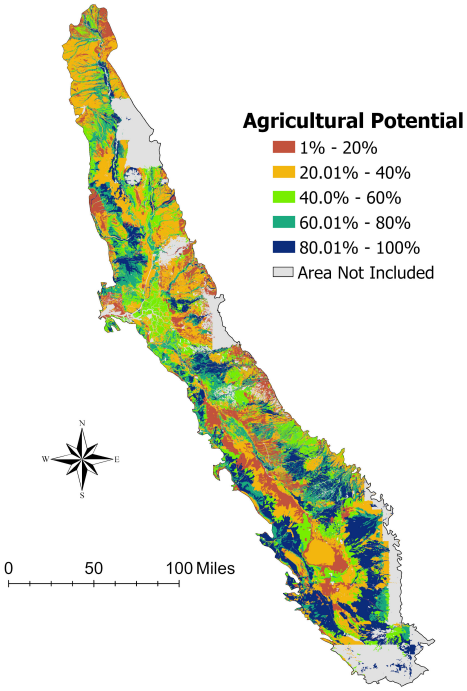

Figure 6: Solar Irradiation

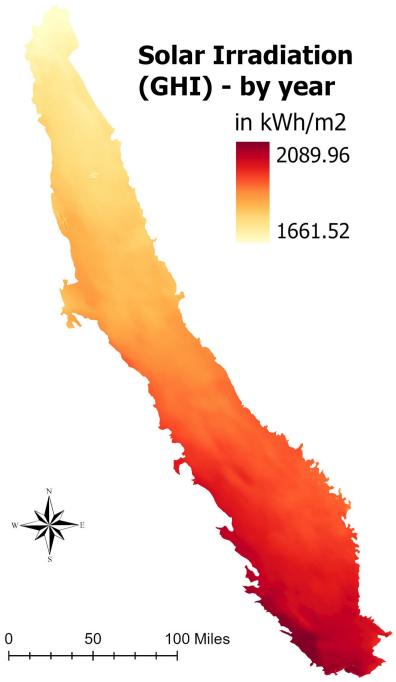

3.6 Solar Irradiation

Average annual solar potential is collected from the Global Solar Atlas (Solargis, 2023), which reports Global Horizontal Irradiance (GHI) in kWh/m² at a 250m resolution, as shown in Figure 6. We normalize GHI to a 0–1 scale to facilitate comparison across parcels. GHI measures the total solar radiation received on a horizontal surface, and is a standard metric for evaluating the energy potential of solar installations. Notably, the average GHI value in the Central Valley is 1,952 kWh/m², exceeding the national average of 1,599 kWh/m².

3.7 Energy Infrastructure

Locations of electricity transmission lines and substations are from the Conservation Biology Institute (2024). This dataset maps major energy infrastructure in California as of 2022 (Figure 7). Distances to transmission lines and substations, plotted in Appendix Figure A1, are calculated as the Euclidean distance from each parcel centroid to the nearest infrastructure point. We invert and log these distances so higher values indicate closer proximity.

Figure 7: Electricity Transmission Infrastructure

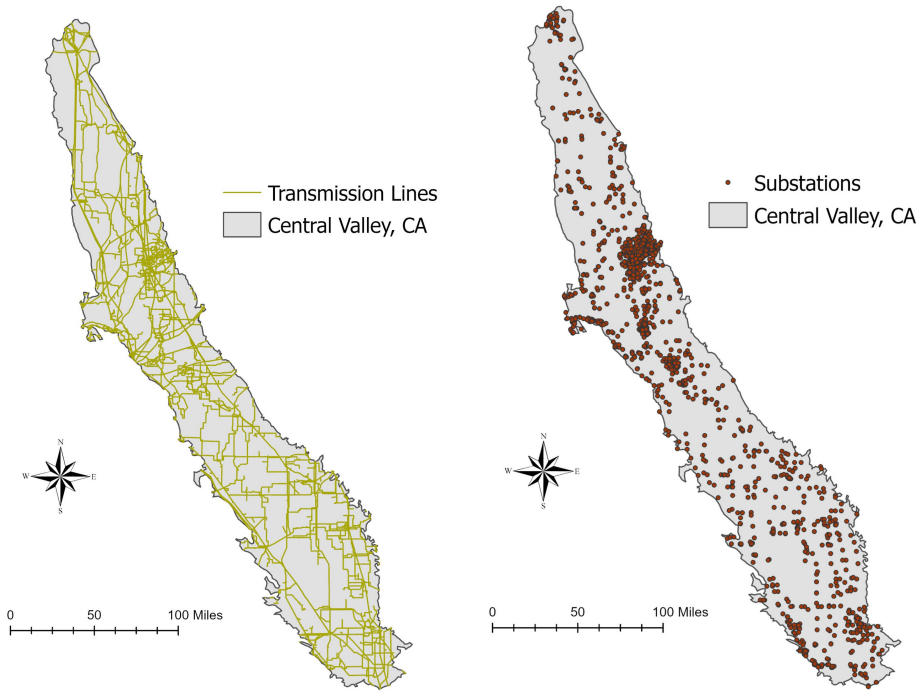

(a) Transmission Lines (b) Substations

3.8 Farm Labor Costs

Finally, we compile data on farm workers' average weekly wages at the county-year level from the Quarterly Census of Employment and Wages (Bureau of Labor Statistics, 2024). We define farm workers using NAICS code 115115 (Farm Labor Contractors and Crew Leaders) and ascribe prevailing wages to all parcels within that county-year, approximating the costs parcel-holders would face when hiring agricultural workers in their local labor market. We deflate nominal wages using the GDP deflator from FRED.

4 Empirical Strategy

We estimate panel regression models to quantify the effects of parcel characteristics on utility-scale solar adoption. In our baseline specification, we regress solar adoption in parcel p and year t on three-year lagged averages of drought severity ($D_{p,t-1:t-3}$) and agricultural labor costs ($L_{p,t-1:t-3}$) and a vector $\mathbf{X}_p$ of time-invariant parcel characteristics (agronomic suitability, solar radiation intensity, proximity to electrical substation and transmission lines, and parcel area), including year fixed effects (δ_t) and clustering standard errors at the parcel level:

$$SolarAdoption_{pt} = \beta D_{p,t-1:t-3} + \gamma L_{p,t-1:t-3} + \mathbf{X}_p'\mu + \delta_t + \epsilon_{pt} \tag{5}$$

$SolarAdoption_{pt}$ denotes either (i) a binary indicator for whether a new solar facility was installed in parcel p in year t (assessing the extensive margin of adoption), or (ii) the total solar-covered area in m^2 (assessing the intensive margin).[5] We estimate all specifications using OLS. For robustness, we re-estimate models with binary adoption outcomes using logit and report marginal effects in Appendix Tables A10-A11 Agricultural labor costs (in deflated real USD), inverse distances (in km) and parcel area (in hectares) are logged.

Given that explanatory variables are measured in different units, direct comparison of coefficient magnitudes is not meaningful. To compare magnitudes, we therefore report standardized coefficient estimates in Appendix Table A6, defined as:

$$\hat{\beta}_j^* = (\hat{\sigma}_j / \hat{\sigma}_y)\hat{\beta}_j \tag{6}$$

where $\hat{\beta}_j$ is the OLS estimator, $\hat{\sigma}_j$ is the sample standard deviation for the j-th explanatory variable, and $\hat{\sigma}_y$ is the sample standard deviation for the dependent variable (solar adoption).

To measure how drought exposure interacts with other parcel characteristics to predict solar adoption, we estimate:

$$SolarAdoption_{pt} = \beta D_{p,t-1:t-3} + \gamma L_{p,t-1:t-3} + \mathbf{X}_p'\mu + (D_{p,t-1:t-3} \times \mathbf{X}_p)'\tau + \delta_t + \epsilon_{pt} \tag{7}$$

This specification allows the effect of drought to vary with parcel characteristics, capturing potential complementarities between environmental stress and other dimensions of solar suit-

[5] We include lagged drought exposure and farm labor costs to test the hypothesis that parcel-holders may update their expectations of future agricultural viability based on their experience of drought and labor costs in prior years. Agriculture in the Central Valley is typically labor intensive, while solar does not require any labor inputs from the parcel-holder. We include three years of lag to account for the typical timeline required to plan, permit, and construct solar facilities (Richardson, 2023).

ability. We also re-estimate this specification including parcel fixed effects (η_p) to absorb potential unobserved time-invariant confounders; in this case, $\mathbf{X}'_p$ is omitted since time-invariant covariates are absorbed by η_p.

Finally, we investigate how prior land cover influences solar adoption. To do so, we include a categorical variable capturing the modal land cover on parcel p in year $t-1$ (i.e., the type of land cover that was replaced by solar on parcels that adopt solar in year t), denoted by a vector of land-use dummies $\mathbf{C}_{p,t-1}$:

$$SolarAdoption_{pt} = \beta D_{p,t-1:t-3} + \gamma L_{p,t-1:t-3} + \mathbf{C}'_{p,t-1}\theta + \mathbf{X}'_p\mu + \delta_t + \epsilon_{pt} \tag{8}$$

The omitted category of $\mathbf{C}_{p,t-1}$ is grassland and pasture, a standard option for solar siting.

4.1 Identification

Our empirical analysis serves two purposes. First, it provides a descriptive characterization of how solar adoption correlates with parcel characteristics, revealing systematic patterns in solar siting. Second, for a subset of variables – particularly drought exposure and labor costs – our research design supports stronger causal interpretations. Year fixed effects (δ_t) absorb time-varying factors common across parcels, including state and federal policy changes and evolving solar technologies. Parcel fixed effects (η_p) absorb time-invariant parcel-level factors, including unobserved owner characteristics insofar as these remain stable over time. Drought exposure is determined by regional climate patterns beyond any landholder's control, making it a plausibly exogenous shock to agricultural profitability. Labor costs are set in regional labor markets and measured at the county level, making individual parcel-holders price takers. Other covariates are better interpreted as predictive correlates. Agronomic suitability is measured at a spatial resolution substantially larger than individual parcels, making it unresponsive to parcel-level management practices, though selection into parcel location could potentially confound these estimates. Distance to transmission infrastructure reflects placement of major substations and transmission lines based on grid-level considerations, though proximity may correlate with unobserved local economic development. Parcel size is fixed over our study period. Prior land use, while strongly predictive of solar adoption, likely reflects both economic fundamentals (e.g., crop profitability) and unobserved landholder characteristics, limiting causal interpretation. Finally, the rapid evolution of solar technology

between 2006 and 2023 means utility-scale solar was not available for most parcel-holders during the early study period. Landholders' initial parcel and crop choices were thus likely taken when solar was not in the feasible choice set, reducing concerns that time-invariant parcel characteristics reflect anticipatory solar-optimizing behavior.

5 Results

There were 215 utility-scale solar energy projects installed across 419 parcels in California's Central Valley between 2006-2023, averaging 52 hectares per project. Figure 8 plots histograms of solar installations across deciles of parcels' (a) drought exposure, (b) solar irradiance, (c) distance to the nearest electrical substation, and (d) agricultural suitability (i.e., soil quality). Histograms for non-solar parcels are plotted in gray outlines for comparison.

Figure 8: Distribution of Solar Siting Across Parcel Characteristics

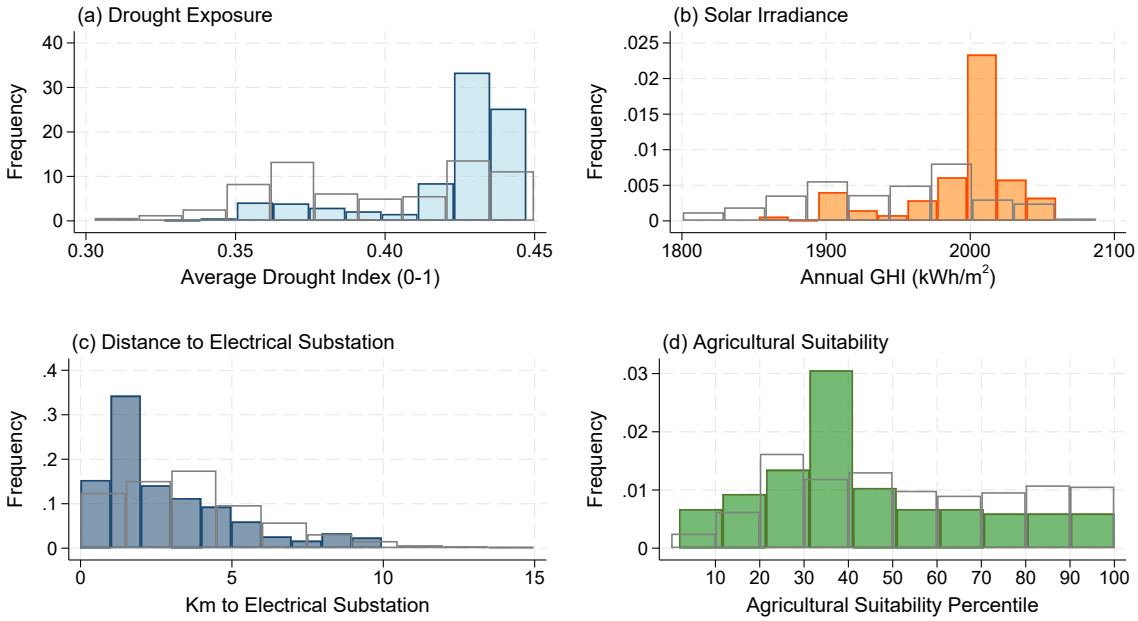

Notes: Panels a-d plot histograms of 419 parcels hosting utility-scale solar facilities (colored bars) compared to 328,781 non-solar parcels (gray outlines) across four parcel characteristics. Panel (a): Average drought exposure index across the 2006-2023 period, normalized to a 0-1 scale. Over 99% of parcels, and all solar parcels, fell within the 0.30-0.45 range. Panel (b): Annual global horizontal irradiance (GHI) in kWh/m^2. Panel (c): Distance to nearest electric substation in kilometers. Over 99% of parcels and all solar parcels were within 15km of a substation. Panel (d): Agricultural suitability measured as percentiles, where higher percentiles indicate higher productivity.

As shown in Figure 8a, solar installations are strongly clustered on parcels with higher average drought exposure between 2006-2023. 71% of solar sites are in the upper quintile of drought severity, with a further 12.2% in the fourth quintile. Non-solar parcels are much more evenly spread across drought exposure. Figure 8b shows that 79% of solar installations are located on parcels in the top two quintiles of solar irradiance. The left tail of solar sites on below-median parcels reflects the fact that solar irradiance throughout the Central Valley exceeds the national average, making solar panels economically viable even in relatively low-irradiation areas. Figure 8c reveals that distance to an electrical substation is a strong determinant of solar siting: 49% of installations are within 2km from a substation, 90% are within 5km, and all are within 10km (mean distance = 2.9km). In contrast, the mean non-solar parcel is 4.1km from a substation. Finally, Figure 8d documents that solar installations are located across the full distribution of agricultural suitability: 69% are on parcels in the bottom half of the suitability distribution, while 31% are on parcels in the top half – including 24% on parcels in the top two quintiles, representing prime agricultural land. However, compared to the distribution of non-solar parcels, solar installations are relatively less concentrated on the most productive land.

Figure 9 reports land area converted to solar between 2007 and 2022 by land use category. The largest conversions occurred from cereal grains (4,100 ha), fallow and idle cropland (3,863 ha), grassland and pasture (1,083 ha), and feed, fiber, and industrial crops (715 ha). Fruits, nuts, vegetables and melons, and especially tree crops are substantially less likely to be converted to solar – consistent with landowners prioritizing the conversion of flexible or low-return acreage for solar development while retaining more profitable crops and sunk investments. Land conversion to solar was negligible prior to 2010, after which solar expanded rapidly, with a peak in 2015 at 1,844 total hectares of land converted. Solar installations slowed over subsequent years before rebounding in 2019 (2,002 ha) and 2020 (2,248 ha). In total, 10,798 ha of land in the Central Valley were converted to solar during the study period: 5,760 ha from actively cultivated agricultural land, 4,950 ha from grassland, pasture, or fallow/idle cropland, and 88 ha from other land uses (e.g., developed land, forest, wetlands). By 2022, solar facilities occupied 0.23% of non-urban land in the Central Valley. Numeric values of land converted to solar per crop type-year are detailed in Appendix Figure A2.

Table 1 presents our main results, quantifying the parcel-level determinants of solar adop-

Figure 9: Crops Replaced by Solar

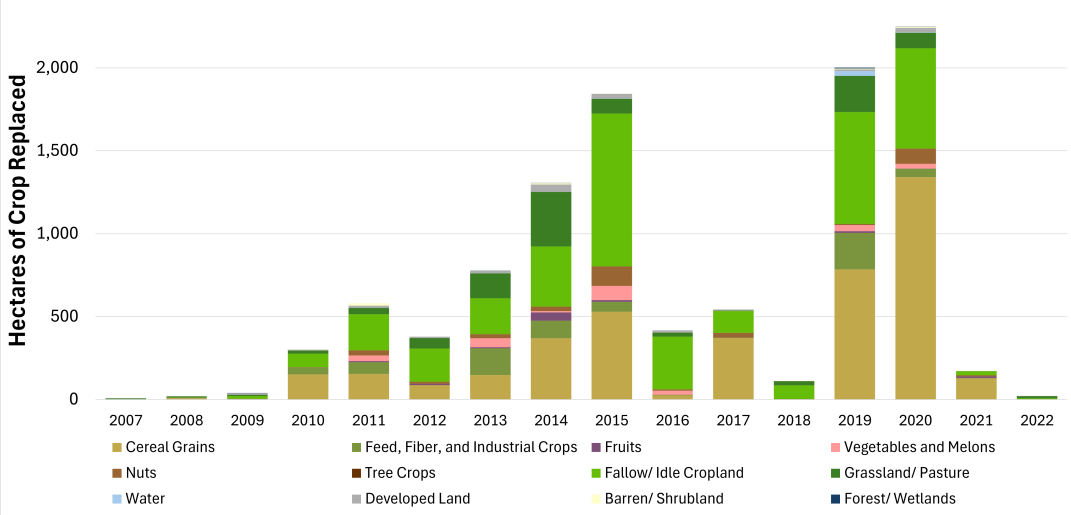

Notes: Crop coverage data are from USDA National Agricultural Statistics Service (2023). Crops included in each category are reported in Appendix Table A1. Areas of each crop type converted to solar are calculated based on crop cover observed in the year prior to solar installation.

tion. The mean adoption probability in our sample is 0.062%. Our baseline specification (column 1) confirms that all hypothesized factors significantly predict solar development. A one-unit increase in the normalized drought index (i.e., moving from no drought to extreme drought) increases the probability of solar adoption by 0.25 percentage points (pp), a fourfold increase relative to mean adoption rate. A one-unit increase in log labor costs (approximately a 2.7-fold increase in labor costs) raises adoption probability by 0.17pp, a nearly threefold increase over the mean. This effect is statistically significant but economically small. Moving from the lowest to highest solar irradiance (within the distribution of the Central Valley – where overall irradiance is high) increases adoption probability by 0.80pp, while a one-unit increase in log inverse distance to substations (equivalent to moving from 5km to 1.8km) increases adoption probability by 0.09pp. Larger parcels are also significantly more likely to adopt solar: a one-unit increase in log area increases adoption probability by 0.03 percentage points. Finally, parcels with poor soil quality are 0.10pp more likely to adopt solar than those with good soil, a 1.6-fold increase relative to the mean adoption rate.

Column 2 reveals that average effects contain substantial heterogeneity. When we include interactions between drought exposure and other parcel characteristics, the main effect of drought becomes negative, indicating that drought alone does not universally increase solar

adoption. Instead, positive interaction terms reveal that effects of drought depend on whether solar development is feasible for a given parcel. Drought exposure increases adoption more on parcels with poor soil quality, high solar irradiance, proximity to a substation, and larger size. Column 3 adds parcel fixed effects to absorb time-invariant parcel characteristics. In this specification, the drought×labor cost interaction becomes significant (0.0029, p<0.01), suggesting that within parcels over time, drought's effect on adoption strengthens as labor costs rise. All other drought interactions remain positive and highly significant.

Table 1: Determinants of Solar Adoption

	Solar Adoption (0/1)		
	Main Effects	**+ Interactions**	**+ Parcel FE**
Drought Exposure (t-1 to t-3)	0.0025***	-0.0131***	-0.0323***
	(0.0004)	(0.0042)	(0.0034)
Labor Cost (log, t-1 to t-3)	0.0017***	0.0012***	0.0017***
	(0.0002)	(0.0001)	(0.0002)
Poor Soil Quality	0.0010***	0.0005***	
	(0.0002)	(0.0001)	
Solar Irradiance	0.0080***	0.0041***	
	(0.0007)	(0.0004)	
Proximity to Substation	0.0009***	0.0003***	
	(0.0001)	(0.0001)	
Parcel Area (log)	0.0003***	0.0001***	
	(0.0000)	(0.0000)	
Drought Interactions			
Drought × Labor Cost		0.0005	0.0029***
		(0.0006)	(0.0004)
Drought × Poor Soil		0.0012***	0.0008***
		(0.0003)	(0.0002)
Drought × Solar Irradiance		0.0099***	0.0115***
		(0.0012)	(0.0012)
Drought × Proximity Substation		0.0016***	0.0013***
		(0.0002)	(0.0002)
Drought × Parcel Area		0.0004***	0.0003***
		(0.0000)	(0.0000)
Year Fixed Effects	Yes	Yes	Yes
Parcel Fixed Effects	No	No	Yes
Mean of Dependent Variable	0.00062	0.00062	0.00062
Observations	3,018,556	3,018,556	3,018,556
Adjusted R-squared	0.00193	0.00211	0.00136
Within R-squared			0.00136

Notes: Table reports linear probability model estimates with robust standard errors clustered at the parcel level in parentheses. Model (1) includes main effects only. Model (2) adds interactions between drought exposure and parcel characteristics. Model (3) includes parcel fixed effects. Distance to transmission lines is included as a control but not shown for brevity (coefficient ≈ 0).
*** $p < 0.01$, ** $p < 0.05$, * $p < 0.1$.

Appendix Table A3 reports analogous estimates using a continuous outcome (installed solar area, in hectares). Results align with LPM results in sign and statistical significance. Point estimates imply that moving from no drought to extreme drought increases installed

area by 0.08ha (i.e., 800 m^2), a one-unit increase in log labor costs increases installed area by 0.06ha, and moving from the lowest to highest solar irradiance increases area by 0.25ha (the largest effect). Interestingly, solar irradiance becomes the dominant predictor on the intensive margin, consistent with installation size being driven by the profitability of additional panels once the decision to install solar has occurred. To analyze the intensive margin explicitly, we restrict the sample to solar-adopting parcels and re-estimate Equation 5 with installed area as the outcome (Appendix Table A4; Appendix Figure A2). Results confirm that solar irradiance is the strongest predictor of how much solar area is installed amongst adopters.

Figure 10 reports standardized coefficients from Table 1, Column 1. Standardized coefficients from all three specifications are reported in Appendix Table A6. These coefficients represent change in solar adoption probability (in standard deviations) resulting from a one standard deviation increase in each predictor, enabling comparison across variables measured in different units. Parcel area emerges as the most important predictor, with a standardized coefficient of approximately 0.03, indicating that a one standard deviation increase in log parcel area is associated with a 0.03 standard deviation increase in probability of solar adoption. Drought exposure is the next largest factor (standardized coefficient = 0.027), followed by proximity to substation (0.025), solar irradiance (0.019), agricultural labor cost (0.015), and poor soil quality (0.012). Proximity to electric transmission lines has the smallest effect (0.005), given that interconnections happen most often at substations rather than the nearest line.

We next explore interaction effects in more detail. Figure 11 plots marginal effects of lagged drought exposure and agricultural labor costs on solar adoption across fixed parcel characteristics. 11a shows that both drought and labor cost effects increase as parcels' soil quality worsens, indicating that threats to agricultural viability from poor soil, drought, and input costs are multiplicative. 11b reveals that drought and labor costs more strongly predict solar adoption on parcels near electrical substations, where lower grid connection costs make solar development feasible and lower cost, tipping the economic balance from agriculture to solar. 11c shows that drought and labor cost effects increase with parcel size, consistent with scale economies favoring larger solar projects. Notably, labor costs have a negative effect on smaller parcels, suggesting that rising agricultural input costs alone do not trigger solar adoption when parcel size is too small to support viable solar facilities. Finally, 11d shows that both drought and labor cost effects strengthen with solar irradiance. Altogether, these

Figure 10: Standardized Coefficients

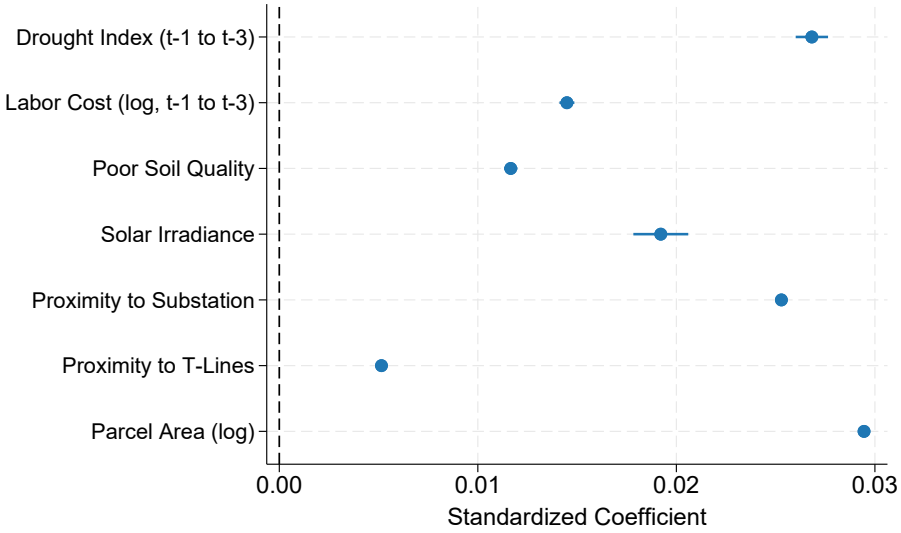

Notes: Figure plots standardized coefficients from Column 1 of Table 1. Each coefficient represents the change in solar adoption probability (in standard deviations) resulting from a one standard deviation increase in the predictor variable. Error bars show 95% confidence intervals based on robust standard errors clustered at the parcel level.

patterns validate our conceptual framework: drought exposure and rising agricultural labor costs accelerate solar adoption specifically on parcels where agricultural returns are declining and solar development is technically feasible and economically attractive.

Finally, we examine how prior land use affects solar adoption. Certain land uses are substantially more valuable than others and may differ in their suitability for conversion to solar. We estimate Equation 8 and plot coefficients for each land use category in Figure 12, with full results reported in Appendix Table A7. The results reveal substantial heterogeneity in conversion propensity across land types. Relative to the reference category (grassland/pasture), fallow and idle cropland is most likely to be converted to solar, followed by developed land (e.g., open space - developed, low-intensity - developed), barren/shrubland, and cereal grains. Excluding developed land, these categories represent relatively flexible or low-value agricultural uses that can be readily repurposed for utility-scale solar without significant clearing or land preparation. In contrast, high-value crops show markedly lower conversion rates: nuts, fruits, feed/fiber/industrial crops (e.g., flaxseed, cotton, sunflower), and vegetables and melons are all substantially less likely to be converted than grassland/pasture. These

Figure 11: Marginal Effects of Drought Exposure and Labor Costs by Parcel Characteristics

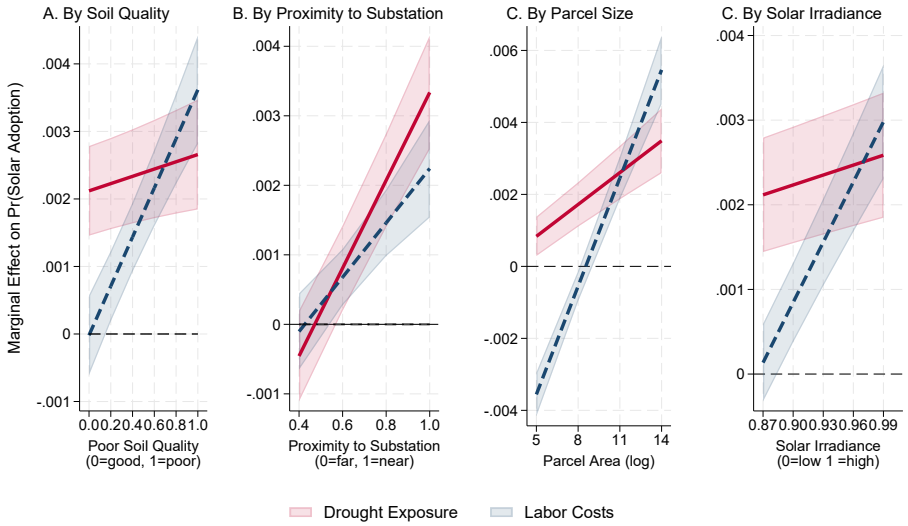

Notes: Figure plots marginal effects of drought exposure and labor costs on solar adoption probability across parcel characteristics, estimated from a linear probability model with both drought and labor cost interactions (similar to Column 2 of Table 1). Panel A varies poor soil quality from 0 (excellent agricultural suitability) to 1 (poor agricultural suitability). Panel B varies proximity to electrical substations from 0.4 (far) to 1 (near), measured as the normalized log inverse distance. Panel C varies log parcel area from 5 to 14. Panel D varies solar irradiance from 0.87 to 1.0 on a normalized scale. Values excluded from these ranges account for less than 1% of the sample and none of the solar parcels. Shaded areas represent 95% confidence intervals based on robust standard errors clustered at the parcel level. All other variables are held at sample means.

patterns demonstrate that solar development does not randomly displace agricultural land, but instead concentrates on parcels with lower opportunity costs, such as those lying fallow, dedicated to low-value annual crops, or supporting livestock grazing.

To assess whether solar serves as an adaptation strategy for lands with declining agricultural productivity, we measure consecutive years each parcel has been fallow or idle. Controlling for drought exposure, labor costs, and other parcel characteristics, solar adoption probability increases sharply with fallow duration: from +0.0017 for parcels that have been fallow for one year to +0.0043 for parcels that have been fallow four or more years (Appendix Figure A3). This pattern confirms that solar development often follows agricultural abandonment.

Figure 12: Effect of Prior Land Use on Solar Adoption

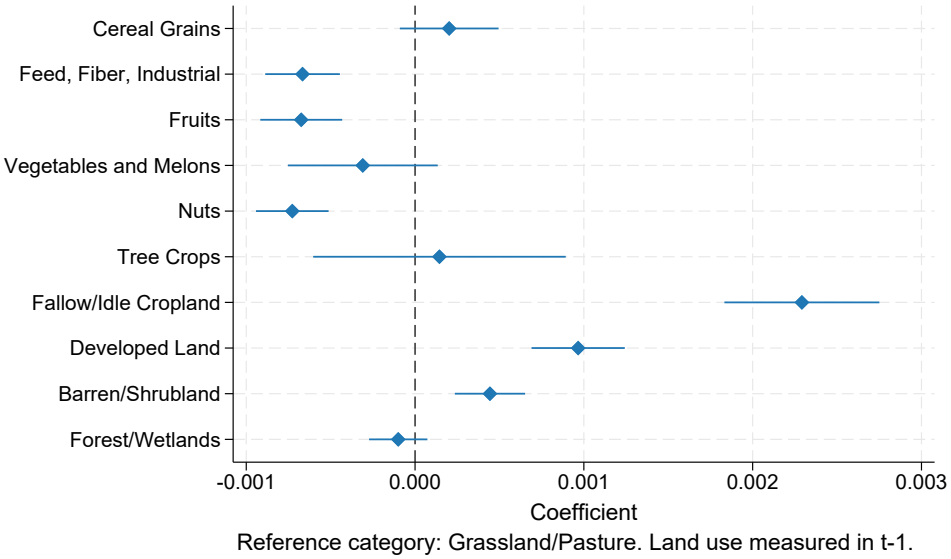

Notes: Figure plots coefficient estimates and 95% confidence intervals from linear probability model showing the effect of prior land use (t-1) on solar adoption probability (Equation 8). The omitted reference land use is grassland/pasture. Water parcels excluded from analysis due to high imprecision in estimates for this category.

5.1 Priority Solar Siting

To prioritize future utility-scale solar development in the Central Valley, we construct a continuous solar suitability index that identifies high-potential parcels that had no solar installation as of 2023. The index applies linear reward and penalty functions over six dimensions: proximity to electric substations, parcel size, drought exposure, solar irradiance, soil quality, and low-value land-use, which are aggregated into a weighted composite based on standardized coefficient estimates from Table 10 and normalized to a 0-100 scale.[6] The distribution of index values is shown in Appendix Figure A4. Figure 13 maps this index for the

[6]Substation proximity is scored at full value at 0km and declines linearly to zero at 4km. Parcel size is scored at zero below 40ha and increases linearly to full value at 200ha. For drought exposure, solar irradiance, and soil quality, we assign scores based on empirical distributions within the study region. Drought exposure receives zero below the 60th percentile, increases linearly from the 60th to the 80th percentile, and reaches full value above the 80th percentile. Solar irradiance receives zero below the 20th percentile, increases linearly from the 20th to 40th percentile, and reaches full value above the 40th percentile, reflecting generally high GHI across the region. Soil quality is scored inversely: parcels receive zero above the 40th percentile, increase linearly from the 40th to the 20th percentile, and receive full value below the 20th percentile. Low-value land uses (defined as grassland/pasture, fallow/idle cropland, developed open space, and barren/scrubland), receive full value; all other land uses receive zero. To incorporate this sixth factor, we re-estimate the standardized coefficient model including the low-value land use indicator, yielding empirically-derived weights for all six components.

Central Valley, revealing clusters of parcels with high solar potential and low agricultural potential – particularly along the Valley's northwest edge and around Chico and Sacramento.[7]

As a conservative targeting rule, we identify high-suitability parcels as those scoring above the 99.9th percentile of the continuous solar suitability index. Appendix Figure A7 maps the resulting 328 parcels, totaling 100,967ha, which could support approximately 25.2GW of generating capacity, or 43.8% of California's 2045 utility-scale solar energy target (Weaver, 2024; CA Public Utilities Commission), while concentrating development on marginal agricultural land with strong solar feasibility in the Central Valley alone.[8]

5.2 Out-of-Sample Validation

To assess predictive power of the suitability index, we conduct an out-of-sample validation exercise. We estimate the model using only data from 2006-2018 and apply the resulting standardized coefficients to 2018 parcel characteristics to generate predicted suitability scores. We then divide all non-solar parcels as of 2018 into deciles based on these predicted scores and examine whether actual solar installations occurring between 2019-2023 concentrate in higher-predicted-suitability deciles. Figure 14 confirms strong out-of-sample predictive power: post-2018 solar adoption rates increase from near-zero in the bottom deciles to 0.12-0.14% in each of deciles 8-10.[9] Notably however, 41% of post-2018 installations (61 of 147) occurred outside the top suitability quintile. While this could reflect unobserved factors such as landholder preferences, it also suggests scope for siting policies that guide development toward parcels with high solar potential and low agricultural opportunity costs.

5.3 Robustness

We conduct a series of robustness checks to assess the stability of our findings. First, we re-estimate linear probability models using alternative lag structures for drought exposure and agricultural labor costs, replacing our preferred 3-year lag with 1-year and 5-year lags.

[7] Appendix Figure A5 presents an alternative simple count index using binary versions of the same criteria. Appendix Figure A6 confirms a strong positive correlation between the two measures.

[8] Megawatt values are calculated based on an assumption of 0.5MW per hectare of solar panels and 50% of parcel area dedicated to panels, which is the sample average.

[9] Appendix Figure A8 confirms this pattern by plotting marginal effects from a logistic regression of post-2018 solar adoption on predicted solar suitability deciles as of 2018, revealing a significant increase in adoption likelihood in the top three deciles. Appendix Figure A9 plots the ROC curve with an area under the curve of 0.803, indicating that the solar suitability index correctly ranks parcels by likelihood of solar adoption 80% of the time.

Figure 13: Continuous Solar Suitability Index

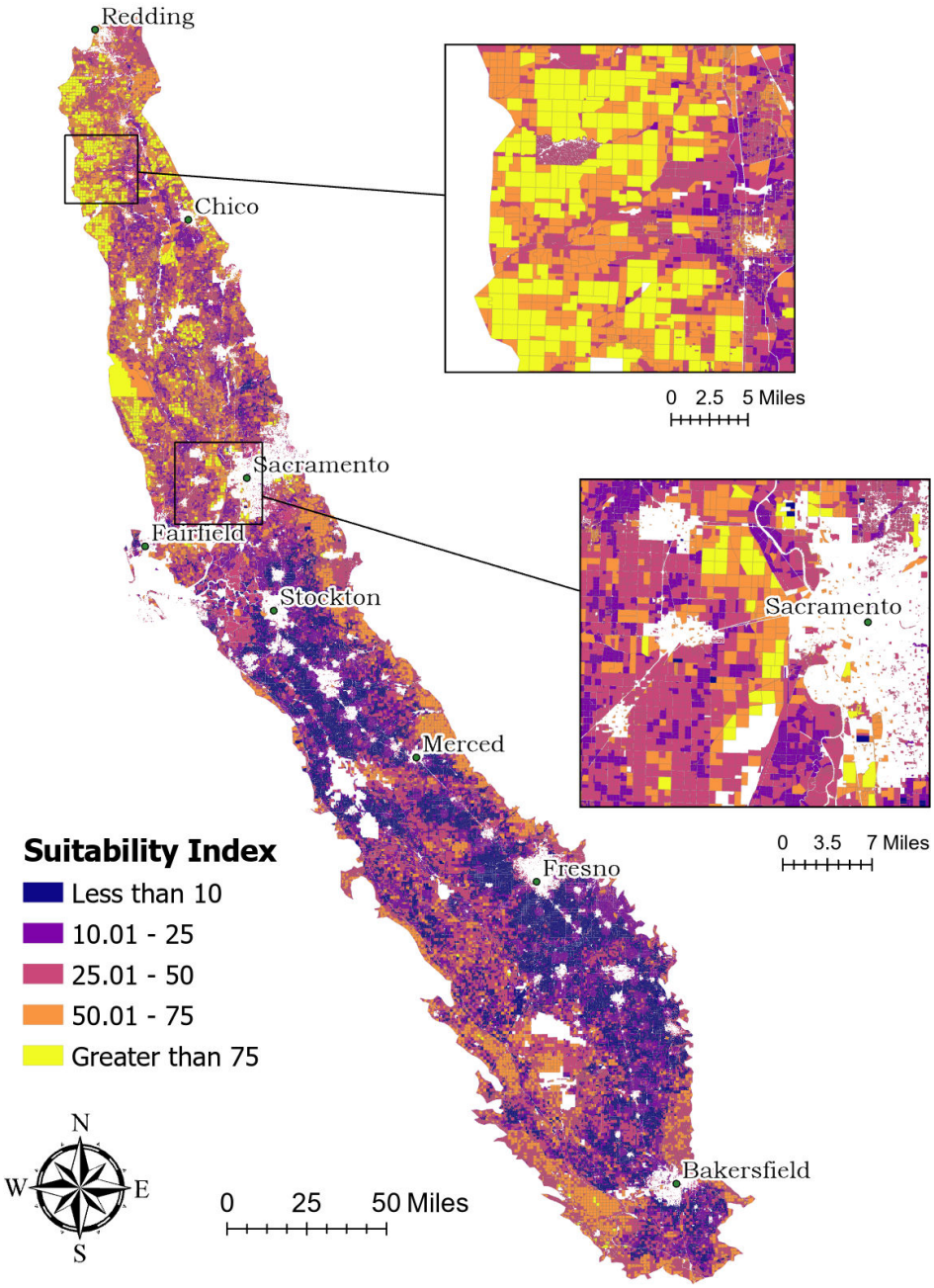

Notes: Map shows the continuous solar suitability index (0-100) for non-urban parcels in California's Central Valley with no solar installation as of 2023. The index combines weighted penalty functions for six characteristics: proximity to electrical substations (full value at 0km, declining linearly to zero at 4km), parcel size (zero below 40ha, full value above 200ha), drought exposure (rewarded above 60th percentile, full value above 80th percentile), solar irradiance (rewarded above 20th percentile, full value above 40th percentile), poor soil quality (rewarded below 40th percentile, full value below 20th percentile), and low-value land use (full value for fallow/idle cropland, grassland/pasture, developed open space, or barren/shrubland; zero otherwise). Weights are based on standardized regression coefficients. Parcels with low/medium/high-density development are set to zero.

Figure 14: Solar Adoption Rate in 2019-2023 by Predicted Suitability Decile

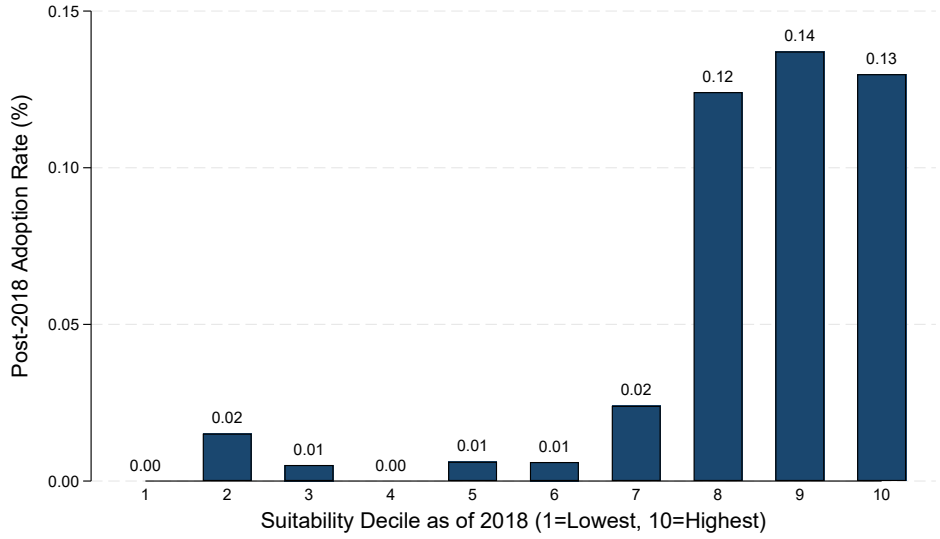

Note: Figure reports solar adoption rates for 2019-2023 by deciles of predicted suitability as of 2018, estimated using 2006-2018 data. Adoption rates indicate the percentage of parcels within each decile that adopted solar after 2018.

The results, reported in Appendix Tables A7 and A8, show smaller effects under the 1-year lag and larger effects under the 5-year lag, consistent with landholders responding more strongly as exposure accumulates over time. Second, we re-estimate our preferred specifications excluding the poor soil quality measure. Because this variable is unavailable for parts of the Central Valley, its inclusion mechanically drops those areas (including 27 solar parcels) from the regression sample. Dropping the soil-quality control leaves the estimates for remaining covariates essentially unchanged (Appendix Table A9). Finally, we re-estimate Equations 5 and 7 using logit and report average marginal effects in Appendix Tables A10 and A11. Logit-estimated effects of prior land-use on solar adoption are plotted in Appendix Figure A10. The logit-based estimates are similar to linear probability model results.

6 Discussion

California's Central Valley is an ideal setting to study land-use tradeoffs arising from the transition to renewable energy. One of the world's most productive agricultural regions, the Central Valley supplies a quarter of U.S. food production, yet faces mounting pressure from

drought and groundwater depletion. Simultaneously, California's emission reduction targets aim for 57.5 gigawatts of new utility-scale solar capacity by 2045, much of which will compete for the same lands that currently support agriculture. The central question is whether solar development threatens agricultural communities or offers an economic lifeline amid changing environmental conditions.

Our findings reveal systematic patterns in utility-scale solar adoption. Consistent with a conceptual framework where landholders choose between agriculture and solar to maximize expected returns from their land, we find that solar adoption concentrates on parcels where agriculture is least viable and solar development is most attractive. Solar adoption increases significantly with parcel-level drought exposure, agricultural labor costs, poor soil quality, solar irradiance, proximity to electrical substations, and parcel size. High-value permanent crops such as nuts are rarely converted, while low-value land uses such as fallow/idle cropland, grassland/pasture, and barren land are disproportionately selected. Applying these criteria to prioritize parcels where solar benefits are high and agricultural opportunity costs are low, we identify 328 optimal sites that could generate 25.2 GW – representing 44% of California's 2045 utility-scale solar target – while concentrating development on agriculturally marginal lands in the Central Valley alone.

This study has several limitations. First, we do not observe landholder characteristics, which could shape solar adoption decisions in ways our parcel-level covariates cannot capture. Second, our framework focuses on individual land-use decisions and does not account for broader community impacts, including effects on agricultural service sectors, local tax revenues, or landscape aesthetics. Solar installations could have mixed effects on neighbors, potentially imposing negative externalities, such as visual impacts, and positive externalities, such as reduced competition for scarce groundwater. Third, we only observe utility-scale solar installations exceeding 1 MW, potentially understating total solar deployment and missing distinct siting patterns for smaller projects.

These findings challenge the view that expansion of utility-scale solar necessarily threatens agricultural communities. Solar adoption concentrates precisely where farming faces the greatest challenges – on drought-exposed, high-cost parcels with poor soil – in line with benefit-maximizing decisions by landholders. This pattern suggests that strategic siting policies can reconcile competing imperatives to expand renewable energy generation while pre-

serving agricultural production in California. More broadly, our results reveal solar leasing as a climate adaptation mechanism that may help sustain rural economies as climate change intensifies, providing stable returns when agricultural viability declines.

References

Elnaz H. Adeh, Stephen P. Good, M. Calaf, and Chad W. Higgins. Solar pv power potential is greatest over croplands. *Scientific Reports*, 9(1), 2019. ISSN 2045-2322. doi: 10.1038/s41598-019-47803-3. URL http://dx.doi.org/10.1038/s41598-019-47803-3.

F.A. Akyuz. Drought severity and coverage index | u.s. drought monitor. https://droughtmonitor.unl.edu/About/AbouttheData/DSCI.aspx, 2017. Accessed: 2025-02-27.

Ellen Hanak John Abatzoglou Alvar Escriva-Bou, Josue Medllin-Azuara and Joshua Viers. Policy brief: Drought and california's agriculture. Technical report, Public Policy Institute of California, 2022.

Stephen Battersby. How to expand solar power without using precious land. *Proceedings of the National Academy of Sciences*, 120(9):e2301355120, 2023. doi: 10.1073/pnas.2301355120. URL https://www.pnas.org/doi/abs/10.1073/pnas.2301355120.

Mark Bolinger and Greta Bolinger. Land requirements for utility-scale pv: An empirical update on power and energy density. *IEEE Journal of Photovoltaics*, 12(2):589–594, 2022. ISSN 2156-3403. doi: 10.1109/jphotov.2021.3136805. URL http://dx.doi.org/10.1109/JPHOTOV.2021.3136805.

Nicole Buckley Biggs, Ranjitha Shivaram, Estefanía Lacarieri, Kavya Varkey, Devin Hagan, Hannah Young, and Eric Lambin. Landowner decisions regarding utility-scale solar energy on working lands: a qualitative case study in california. *Environmental Research Communications*, 4, 2022. doi: 10.1088/2515-7620/ac6fbf.

Bureau of Labor Statistics. Quarterly census of employment and wages. https://www.bls.gov/cew/, 2024. U.S. Department of Labor. Retrieved December 2024.

CA Public Utilities Commission. Decision adopting 2023 preferred system plan and related matters, and addressing two petitions for modification. Decision D.24-02-047, California Public Utilities Commission, San Francisco, CA. URL https://docs.cpuc.ca.gov/PublishedDocs/Published/G000/M525/K918/525918033.PDF. Adopted February 15, 2024. Rulemaking 20-05-003.

Hoy F. Carman. California's changing land use patterns for crop production, 1959-2017. Technical report, University of California Giannini Foundation of Agricultural Economics, 2019.

CEC. Renewable portfolio standard, 2021a.

CEC. Sb 100 joint agency report, 2021b.

Hrishikesh A. Chandanpurkar, James S. Famiglietti, Kaushik Gopalan, David N. Wiese, Yoshihide Wada, Kaoru Kakinuma, John T. Reager, and Fan Zhang. Unprecedented continental drying, shrinking freshwater availability, and increasing land contributions to sea level rise. *Science Advances*, 11(30):eadx0298, 2025. doi: 10.1126/sciadv.adx0298.

Conservation Biology Institute. Databasin: Datasets. https://databasin.org/, 2024. Platform that post-processed and hosted soil data information from SSURGO and NRCS.

Thomas L. Daniels. The development of utility-scale solar projects on us agricultural land: opportunities and obstacles. *Socio-Ecological Practice Research*, 5(2):205–213, 2023. ISSN 2524-5287. doi: 10.1007/s42532-023-00139-9. URL http://dx.doi.org/10.1007/s42532-023-00139-9.

Tom Daniels and Hannah Wagner. Regulating utility-scale solar project on agricultural land. Technical report, University of Pennsylvania, 2022.

Richard Howitt Peter Moyle Brian Gray Josué Medellín-Azuara Sarge Green Thomas Harter Nathaniel Seavy Alvar Escriva-Bou Brad Arnold Ellen Hanak, Jay Lund and Duncan MacEwan. Water stress and a changing san joaquin valley. Technical report, Public Policy Institute of California, 2017.

Michael J. Evans, Kumar Mainali, Rachel Soobitsky, Emily Mills, and Susan Minnemeyer. Predicting patterns of solar energy buildout to identify opportunities for biodiversity conservation. *Biological Conservation*, 283:110074, 2023. ISSN 0006-3207. doi: 10.1016/j.biocon.2023.110074. URL http://dx.doi.org/10.1016/j.biocon.2023.110074.

K.S. Fujita, Z.H. Ancona, L.A. Kramer, M. Straka, T.E. Gautreau, C.P. Garrity, D. Robson, J.E. Diffendorfer, and B. Hoen. United states large-scale solar photovoltaic database (v2.0, august, 2024). https://doi.org/10.5066/P9IA3TUS, 2023.

Zachary A. Goldberg. Solar energy development on farmland: Three prevalent perspectives of conflict, synergy and compromise in the united states. *Energy Research amp; Social Science*, 101:103145, 2023. ISSN 2214-6296. doi: 10.1016/j.erss.2023.103145. URL http://dx.doi.org/10.1016/j.erss.2023.103145.

Rebecca R. Hernandez, Madison K. Hoffacker, Michelle L. Murphy-Mariscal, Grace C. Wu, and Michael F. Allen. Solar energy development impacts on land cover change and protected areas. *Proceedings of the National Academy of Sciences*, 112(44):13579–13584, 2015. ISSN 1091-6490. doi: 10.1073/pnas.1517656112. URL http://dx.doi.org/10.1073/pnas.1517656112.

Madison K. Hoffacker, Michael F. Allen, and Rebecca R. Hernandez. Land-sparing opportunities for solar energy development in agricultural landscapes: A case study of the great central valley, ca, united states. *Environmental Science amp; Technology*, 51(24):14472–14482, 2017. ISSN 1520-5851. doi: 10.1021/acs.est.7b05110. URL http://dx.doi.org/10.1021/acs.est.7b05110.

IEA. Renewables 2024, 2024. URL https://www.iea.org/reports/renewables-2024.

Camille Von Kaenel and Wes Venteicher. A new survival strategy for central valley farmers. https://www.politico.com/newsletters/california-climate/2024/10/29/a-new-survival-strategy-for-central-valley-farmers-00186175, 2024. [Accessed 04-05-2025].

LACounty. California statewide parcel boundaries egis-lacounty.hub.arcgis.com. https://egis-lacounty.hub.arcgis.com/documents/baaf8251bfb94d3984fb58cb5fd93258/about, 2025. [Accessed 06-05-2025].

Lazard. Lazard levelized cost of energy+, 2025. URL https://www.lazard.com/media/uounhon4/lazards-lcoeplus-june-2025.pdf. Accessed: 2025-07-29.

Solar Land Lease. How does a solar farm connect to the grid? https://www.solarlandlease.com/solar-farm-connect-grid, 2022. [Accessed 04-04-2025].

P. W. Liu, J. S. Famiglietti, A. J. Purdy, et al. Groundwater depletion in california's central valley accelerates during megadrought. *Nature Communications*, 13(7825), 2022. doi: 10.1038/s41467-022-35582-x.

J. Medellín-Azuara, R.E. Howitt, and J.J. Harou. Predicting farmer responses to water pricing, rationing and subsidies assuming profit maximizing investment in irrigation technology. *Agricultural Water Management*, 108:73–82, May 2012. ISSN 0378-3774. doi: 10.1016/j.agwat.2011.12.017. URL http://dx.doi.org/10.1016/j.agwat.2011.12.017.

Sharlissa Moore, Hannah Graff, Carolyn Ouellet, Skyler Leslie, and Danny Olweean. Can we have clean energy and grow our crops too? solar siting on agricultural land in the united states. *Energy Research and Social Science*, 91, 07 2022. ISSN ISSN 2214-6296. doi: 10.1016/j.erss.2022.102731. URL https://www.osti.gov/biblio/1887217.

Jeffrey Mount and Ellen Hanak. Water use in california. Technical report, Public Policy Institute of California, 2019.

Natural Resources Conservation Service. Gridded soil survey geographic (gssurgo) database for california. https://databasin.org/datasets/899148f7939b40d2bbac3b1647dd9de5, 2022. United States Department of Agriculture, Natural Resources Conservation Service. Post-processed by Conservation Biology Institute.

Alexis S. Pascaris, Chelsea Schelly, Laurie Burnham, and Joshua M. Pearce. Integrating solar energy with agriculture: Industry perspectives on the market, community, and socio-political dimensions of agrivoltaics. *Energy Research amp; Social Science*, 75:102023, 2021. ISSN 2214-6296. doi: 10.1016/j.erss.2021.102023. URL http://dx.doi.org/10.1016/j.erss.2021.102023.

Valley Clean Infrastructure Plan. About the vcip. https://valleycleaninfrastructureplan.com/about-vcip/, 2025.

Mark Richardson. How long does it take to build a solar farm? process explained. https://uslightenergy.com/how-long-does-it-take-to-build-a-solar-farm/, 2023. Accessed: 2025-06-05.

Nathaly M. Rivera, J. Cristobal Ruiz-Tagle, and Elisheba Spiller. The health benefits of solar power generation: Evidence from chile. *Journal of Environmental Economics and Management*, 126:102999, 2024. ISSN 0095-0696. doi: https://doi.org/10.1016/j.jeem.2024.102999. URL https://www.sciencedirect.com/science/article/pii/S0095069624000731.

Solargis. Global horizontal irradiation (ghi) gis data - global solar atlas. https://globalsolaratlas.info, 2023. World Bank Group, Energy Sector Management Assistance Program (ESMAP).

Jacob Stid, Siddharth Shukla, Anthony Kendall, Annick Anctil, David Hyndman, Jeremey Rapp, and Robert Anex. Impacts of agrisolar co-location on the food–energy–water nexus and economic security. *Nature Sustainability*, 8:702–713, 2025. doi: https://doi.org/10.1038/s41893-025-01546-4.

Jacob T. Stid, Siddharth Shukla, Annick Anctil, Anthony D. Kendall, Jeremy Rapp, and David W. Hyndman. Solar array placement, electricity generation, and cropland displacement across california's central valley. *Science of The Total Environment*, 835:155240, 2022. ISSN 0048-9697. doi: 10.1016/j.scitotenv.2022.155240. URL http://dx.doi.org/10.1016/j.scitotenv.2022.155240.

University of Nebraska–Lincoln. Gis data | u.s. drought monitor. https://droughtmonitor.unl.edu/DmData/GISData.aspx, 2025. Accessed: 2025-02-15.

USDA National Agricultural Statistics Service. Crop data layer for california [gis datafset]. https://croplandcros.scinet.usda.gov/, 2023. Accessed: 2025-06-09.

USGS. California's central valley | usgs california water science center. https://ca.water.usgs.gov/projects/central-valley/about-central-valley.html, 2023. Accessed April 28, 2025.

M. Anne Visser, Grace Kumetat, and Gwendolyn Scott. Drought, water management, and agricultural livelihoods: Understanding human-ecological system management and livelihood strategies of farmer's in rural california. *Journal of Rural Studies*, 109:103339, 2024. ISSN 0743-0167. doi: 10.1016/j.jrurstud.2024.103339. URL http://dx.doi.org/10.1016/j.jrurstud.2024.103339.

A. C. Wartenberg, D. Moanga, and V. Butsic. Identifying drivers of change and predicting future land-use impacts in established farmlands. *Journal of Land Use Science*, 17(1):161–180, 2021. ISSN 1747-4248. doi: 10.1080/1747423x.2021.2018061. URL http://dx.doi.org/10.1080/1747423X.2021.2018061.

John Fitzgerald Weaver. California needs 10 gw of annual solar deployment in five years, 57.5 gw of new solar added by 2045. pv magazine USA, 2024. URL https://pv-magazine-usa.com/2024/02/26/california-needs-10-gw-of-annual-solar-deployment-in-five-years-57-5-gw-annually-by-2045/. Published February 26, 2024. Accessed February 8, 2026.

ONLINE APPENDIX

Table A1: Reclassification of Crop Categories

New Classification	Old Classification
Cereal Grains	Corn, Rice, Sorghum, Soybeans, Barley, Durum Wheat, Spring Wheat, Other Small Grains, Rye, Oats, Milet, Speltz, Buckwheat, Lentils, Triticale, Dbl Crop WinWht/Soybeans, Dbl Crop WinWht/Corn, Dbl Crop Oats/Corn, Dbl Crop Barley/Sorghum, Dbl Crop WinWht/Sorghum, Dbl Crop Barley/Corn, Dbl Crop WinWht/Cotton
Feed, Fiber, and Industrial Crops	Flaxseed, Cotton, Sunflower, Canola, Safflower, Alfalfa, Other Hay/ Non Alfalfa, Camelina, Sugarcane, Hops, Clover/Wildflowers, Sod/Grass Seed, Tobacco, Dry Beans, Other Crops
Fruits	Mint, Caneberries, Cherries, Peaches, Apples, Grapes, Citrus, Pears, Prunes, Oranges, Pomegranates, Nectarines, Plums, Strawberries, Apricots, Blueberries, Cranberries
Vegetables and Melons	Mustard, Sweet Corn, Pop or Orn Corn, Sugarbeets, Potatoes, Sweet Potatoes, Misc Vegs and Fruits, Watermelons, Onions, Cucmbers, Chick Peas, Peas, Tomaties, Herbs, Carrots, Asparagus, Garlic, Cantaloupes, Olives, Honeydew Melons, Broccoli, Peppers, Greens, Squash, Vetch, Lettuce, Pumpkins, Cabbage, Cauliflower, Celery, Radishes, Turnips
Nuts	Peanuts, Almonds, Walnuts, Pecans, Pistachios
Tree Crops	Christmas Trees, Other Tree Crops
Fallow/ Idle Cropland	Fallow/ Idle Cropland
Grassland/ Pasture	Switchgrass, Grassland/ Pasture
Water	Aquaculture, Open Water, Perennial Ice/ Snow
Developed Land	Developed/ Open Space, Developed/ Low Intensity, Developed/ Med Intensity, Developed/ High Intensity
Barren/ Shrubland	Shrubland, Barren
Forest/ Wetlands	Forest, Wetlands, Deciduous Forest, Evergreen Forest, Mixed Forest, Woody Wetlands, Herbaceous Wetlands

Figure A1: Parcel Distance from Electrical Transmission Lines and Substations

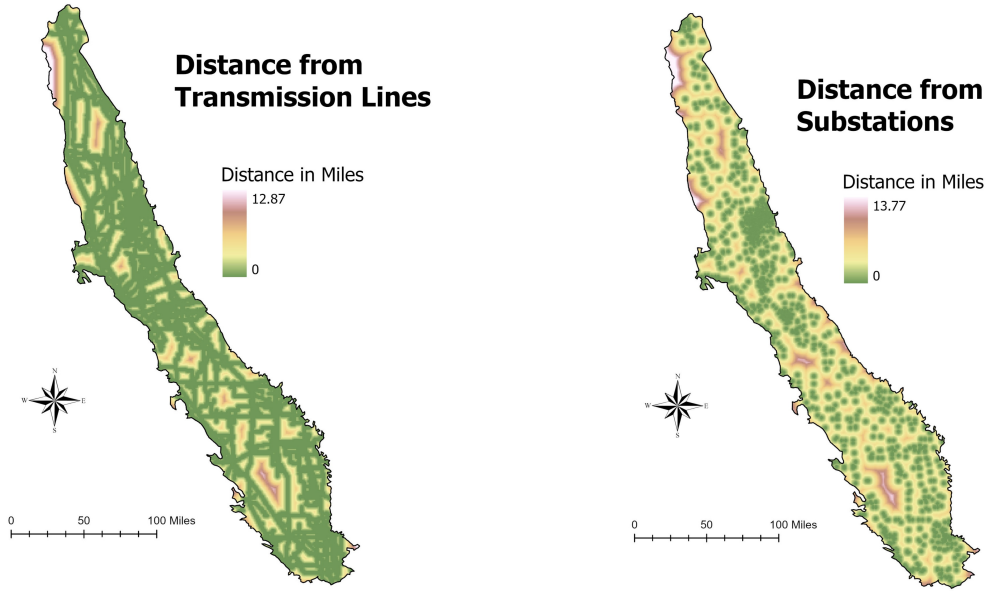

Table A2: Crops Replaced by Solar (in hectares), 2007–2022

Year	Cereal Grains	Feed, Fiber & Industrial Crops	Fruits	Vegetables & Melons	Nuts	Tree Crops	Fallow/Idle Cropland	Grassland & Pasture	Water	Developed Land	Barren/ Shrubland	Forest/ Wetlands
2007	0.82	0.00	0.00	0.00	0.00	0.00	0.00	6.32	0.00	1.26	0.00	0.00
2008	7.33	0.50	1.08	0.56	0.57	0.00	2.51	6.22	0.04	2.13	0.12	0.00
2009	0.77	0.08	1.70	0.00	1.70	0.00	17.03	7.37	0.00	9.86	0.00	0.15
2010	151.73	42.51	0.11	0.16	0.21	0.00	81.15	18.83	0.00	6.67	0.43	0.00
2011	155.27	69.06	7.88	32.75	32.14	0.00	217.35	38.07	0.11	13.21	15.17	0.00
2012	86.59	0.78	7.67	0.00	11.72	0.02	200.53	64.49	0.00	7.20	0.00	0.00
2013	147.96	161.60	6.70	54.18	24.06	0.00	216.04	150.54	0.00	14.35	0.65	1.28
2014	369.81	105.01	50.87	7.83	27.23	0.00	363.23	327.98	0.04	45.20	7.79	1.72
2015	529.56	58.97	11.54	85.44	116.73	0.03	922.76	88.83	1.02	29.50	0.75	0.00
2016	24.07	4.13	0.46	24.20	7.87	0.00	319.17	23.32	0.00	10.94	0.06	0.11
2017	371.75	0.39	0.00	0.00	30.60	0.00	130.99	2.10	0.00	7.25	0.00	0.00
2018	0.03	0.18	0.00	0.00	0.14	2.68	83.18	24.75	0.00	0.80	0.32	0.00
2019	785.95	219.05	9.84	37.56	6.66	0.26	674.37	218.00	29.13	10.79	4.72	5.96
2020	1,341.46	49.98	1.86	28.84	91.17	0.00	605.41	92.99	3.38	26.35	5.60	0.52
2021	126.95	3.14	10.20	0.00	6.41	0.01	23.50	0.52	0.00	1.92	0.03	0.00
2022	0.15	0.05	0.00	0.00	1.17	0.00	5.97	13.04	0.00	0.46	0.00	0.00
Total	**4,100.21**	**715.41**	**109.91**	**271.51**	**358.40**	**2.99**	**3,863.17**	**1,083.38**	**33.72**	**187.89**	**35.65**	**9.74**

Figure A2: Intensive Margin: Solar Area (Ha) on Adopting Parcels

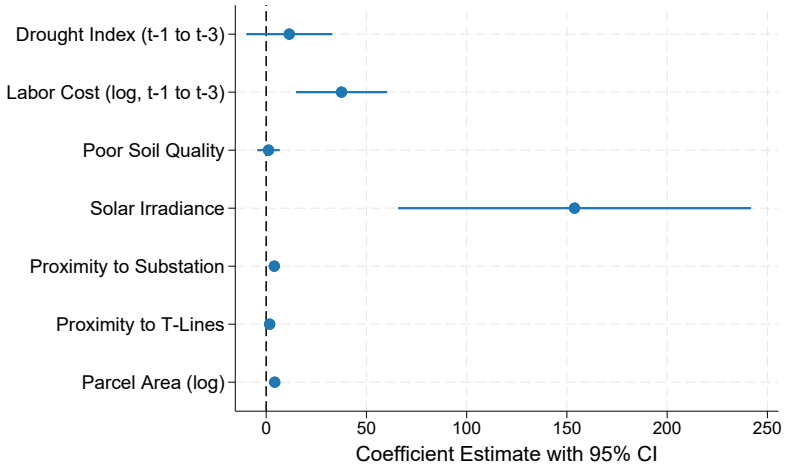

Notes: Coefficient plot from logit model showing the effect of prior land use (t-1) on solar adoption probability. Points represent marginal effects with 95% confidence intervals. Reference category: Grassland/Pasture. Water parcels excluded from analysis. Robust standard errors clustered at the parcel level.

Table A3: OLS: Solar Area (Ha)

	Solar Adoption (Ha)		
	(1)	(2)	(3)
Drought Exposure (t-1 to t-3)	0.08***	-0.53***	-1.04***
	(0.02)	(0.15)	(0.16)
Labor Cost (log, t-1 to t-3)	0.06***	0.04***	0.05***
	(0.01)	(0.01)	(0.01)
Poor Soil Quality	0.04***	0.02***	
	(0.01)	(0.00)	
Solar Irradiance	0.25***	0.13***	
	(0.03)	(0.02)	
Proximity to Substation	0.02***	0.01***	
	(0.00)	(0.00)	
Proximity to T-Lines	0.01***	0.00***	
	(0.00)	(0.00)	
Parcel Area (log)	0.01***	0.01***	
	(0.00)	(0.00)	
Interactions			
Drought × Labor Cost		0.03	0.10***
		(0.02)	(0.02)
Drought × Poor Soil Quality		0.04***	0.03***
		(0.01)	(0.01)
Drought × Solar Irradiance		0.30***	0.33***
		(0.05)	(0.05)
Drought × Proximity Substation		0.04***	0.03***
		(0.01)	(0.01)
Drought × Proximity T-Lines		0.01**	0.01
		(0.00)	(0.00)
Drought × Parcel Area (log)		0.01***	0.01***
		(0.00)	(0.00)
Year Fixed Effects	Yes	Yes	Yes
Parcel Fixed Effects	No	No	Yes
Observations	3,018,556	3,018,556	3,018,556
Adjusted R-squared	0.00118	0.00129	0.00058

Notes: Table reports OLS estimates with robust standard errors clustered at the parcel level in parentheses. The outcome is square meters of solar installed. Model (1) includes main effects only. Model (2) adds interactions between drought exposure and parcel characteristics. Model (3) includes parcel fixed effects.
*** $p < 0.01$, ** $p < 0.05$, * $p < 0.1$.

Table A4: OLS: Solar Adoption (^{2})

	Solar Adoption (^{2})
	(1)
Drought Exposure (t-1 to t-3)	11.53
	(10.90)
Labor Cost (log, t-1 to t-3)	37.59***
	(11.54)
Poor Soil Quality	1.18
	(2.85)
Solar Irradiance	153.80***
	(44.70)
Proximity to Substation	4.06***
	(1.18)
Proximity to T-Lines	1.74
	(1.22)
Parcel Area (log)	4.28***
	(0.56)
Year Fixed Effects	Yes
Parcel Fixed Effects	No
Observations	4,509
Adjusted R-squared	0.26811

Notes: Table reports OLS estimates with robust standard errors clustered at the parcel level in parentheses. The outcome is square meters of solar installed. Model (1) includes main effects only.
*** $p < 0.01$, ** $p < 0.05$, * $p < 0.1$.

Table A5: Impact of Prior Land Use on Solar Adoption

	Solar Adoption (0/1)
Drought Exposure (t-1 to t-3)	0.0019***
	(0.0004)
Labor Cost (log, t-1 to t-3)	0.0019***
	(0.0002)
Poor Soil Quality	0.0006***
	(0.0002)
Solar Irradiance	0.0075***
	(0.0007)
Proximity to Substation	0.0009***
	(0.0001)
Proximity to T-Lines	0.0002***
	(0.0001)
Parcel Area (log)	0.0004***
	(0.0000)
Land Use (t-1)	
Cereal Grains	0.0002
	(0.0001)
Feed, Fiber, Industrial Crops	-0.0007***
	(0.0001)
Fruits	-0.0007***
	(0.0001)
Vegetables and Melons	-0.0003
	(0.0002)
Nuts	-0.0007***
	(0.0001)
Tree Crops	0.0001
	(0.0004)
Fallow/Idle Cropland	0.0023***
	(0.0002)
Developed Land	0.0010***
	(0.0001)
Barren/Shrubland	0.0004***
	(0.0001)
Forest/Wetlands	-0.0001
	(0.0001)
Year Fixed Effects	Yes
Parcel Fixed Effects	No
Observations	2,848,684
Adjusted R-squared	0.00305

Notes: Table reports linear probability model estimates with robust standard errors clustered at the parcel level in parentheses. Land use categories are measured in year t-1 (prior to potential solar adoption). The omitted reference category is Grassland/Pasture. Water parcels excluded from the analysis.
*** $p < 0.01$, ** $p < 0.05$, * $p < 0.1$.

Figure A3: Effect of Fallow Duration on Solar Adoption

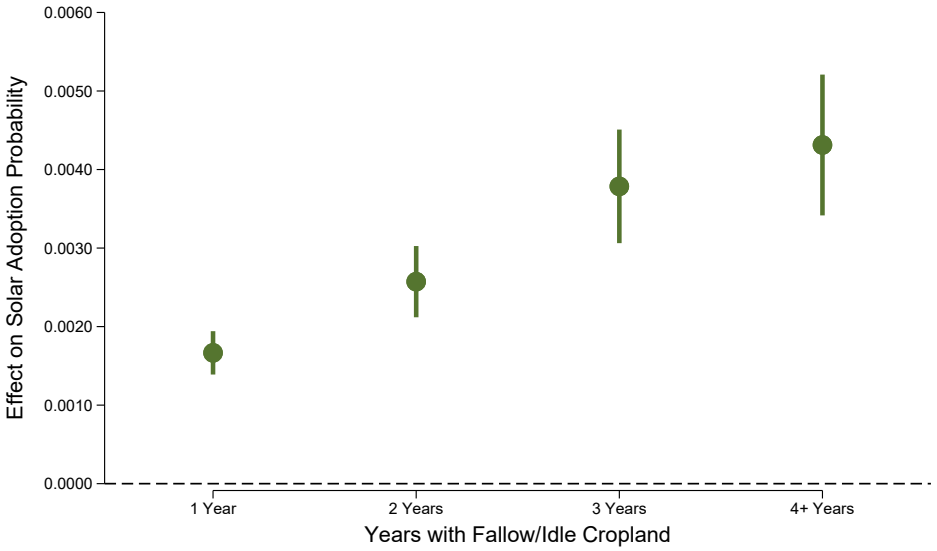

Note: Figure reports coefficient estimates with 95% confidence intervals from a linear probability model showing the effect of fallow/idle cropland duration on solar adoption probability. The reference category consists of parcels that are not currently fallow/idle. Fallow duration is measured as consecutive years in fallow/idle status at t-1 through t-4 or more. The model includes controls for drought exposure, agricultural labor costs, soil quality, solar irradiance, proximity to electrical substations, parcel size, and year fixed effects. Standard errors are clustered at the parcel level.

Table A6: Standardized Coefficients from Linear Probability Model

	Solar Adoption (0/1)		
	(1)	(2)	(3)
Drought Exposure (t-1 to t-3)	0.0268***	-0.1433***	-0.3532***
	(0.0004)	(0.0042)	(0.0034)
Labor Cost (log, t-1 to t-3)	0.0145***	0.0104***	0.0149***
	(0.0002)	(0.0001)	(0.0002)
Poor Soil Quality	0.0117***	0.0059***	
	(0.0002)	(0.0001)	
Solar Irradiance	0.0192***	0.0098***	
	(0.0007)	(0.0004)	
Proximity to Substation	0.0253***	0.0076***	
	(0.0001)	(0.0001)	
Proximity to TLines	0.0051***	0.0029***	
	(0.0001)	(0.0000)	
Parcel Area (log)	0.0295***	0.0137***	
	(0.0000)	(0.0000)	
Interactions			
Drought × Labor Cost		0.0011*	0.0063***
		(0.0006)	(0.0004)
Drought × Poor Soil Quality		0.0035***	0.0023***
		(0.0003)	(0.0002)
Drought × Solar Irradiance		0.0060***	0.0069***
		(0.0012)	(0.0012)
Drought × Proximity Substation		0.0110***	0.0091***
		(0.0002)	(0.0002)
Drought × Proximity T-Lines		0.0014***	0.0002**
		(0.0001)	(0.0001)
Drought × Parcel Area (log)		0.0097***	0.0074***
		(0.0000)	(0.0000)
Year Fixed Effects			
Parcel Fixed Effects			
Observations			
Adjusted R-squared			

Notes: Table reports standardized coefficients from linear probability model with robust standard errors clustered at the parcel level in parentheses. Coefficients are standardized by multiplying the original coefficient by the ratio of the standard deviation of the independent variable to the standard deviation of the dependent variable, allowing comparison of relative importance across variables measured in different units. Model (1) includes main effects only. Model (2) adds interactions between drought exposure and parcel characteristics. Model (3) includes parcel fixed effects.
*** $p < 0.01$, ** $p < 0.05$, * $p < 0.1$.

Figure A4: Distribution of Solar Suitability Scores

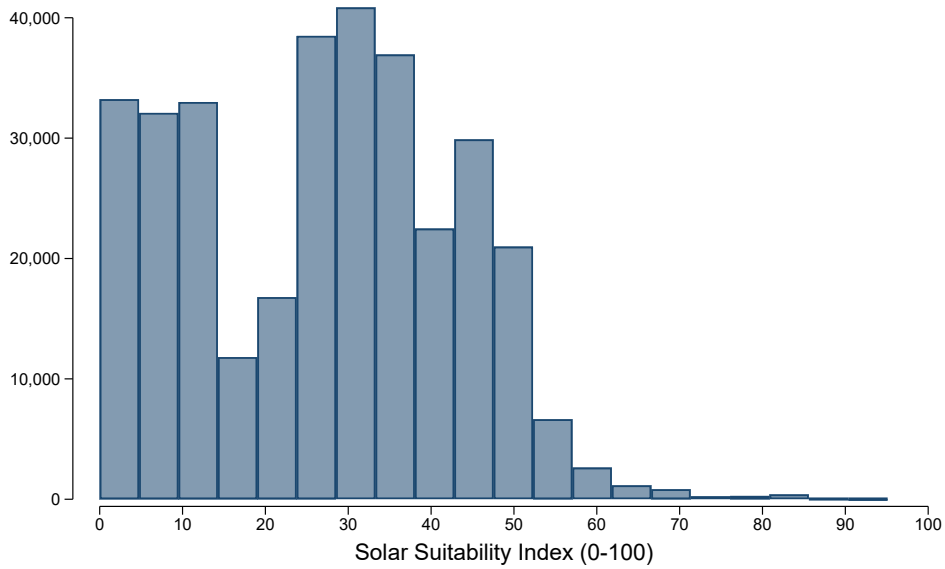

Notes: Histogram shows the distribution of solar suitability scores for non-solar parcels in California's Central Valley. The suitability index (0-100) is a weighted composite of five factors: proximity to electrical substations, parcel size, drought exposure, solar irradiance, and poor soil quality. Higher scores indicate parcels that are both technically suitable for solar development and economically marginal for agriculture.

Figure A5: Simple Solar Suitability Index

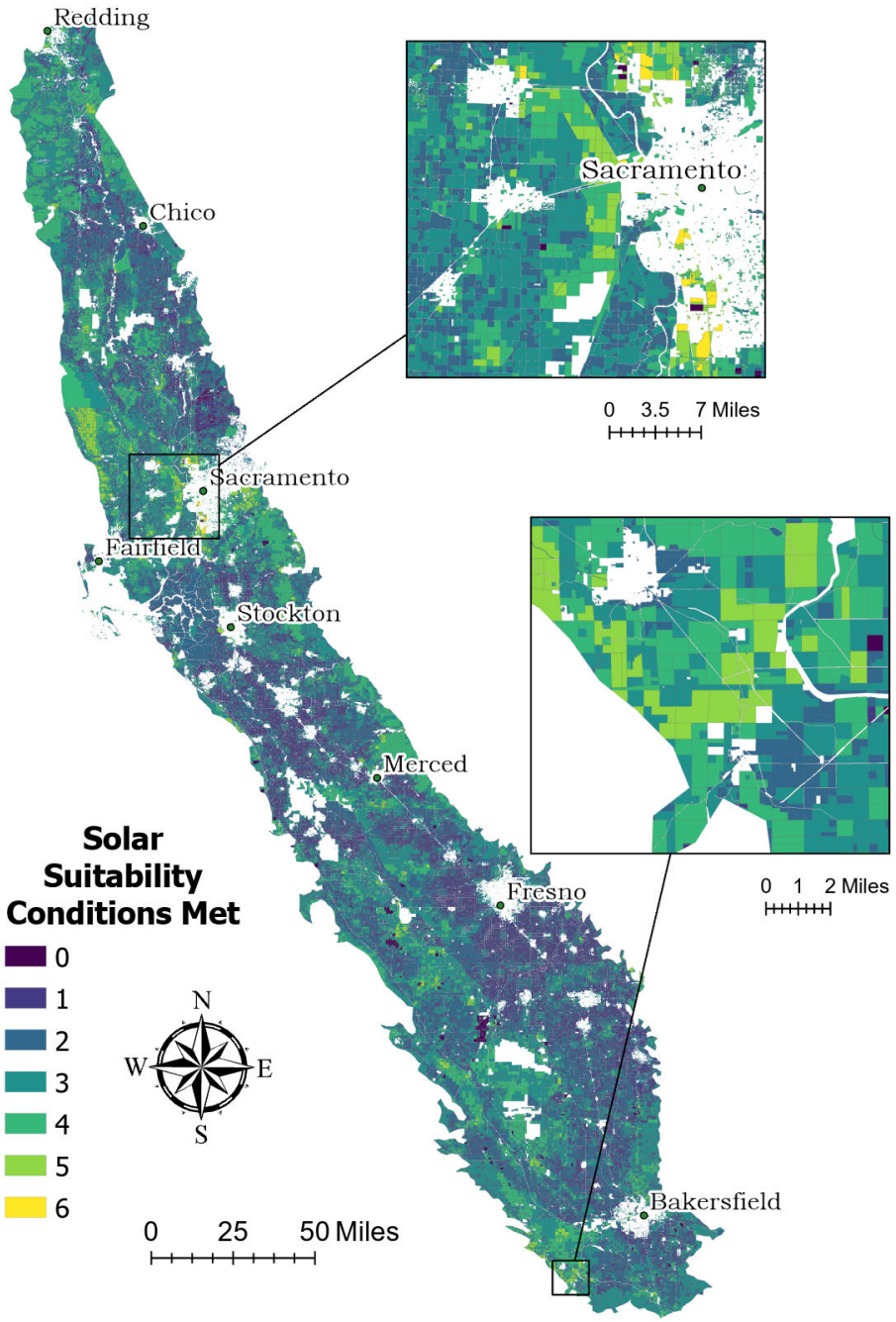

Notes: Map shows a simple solar suitability index (0-6) for non-urban parcels with no solar installation as of 2023, counting the number of favorable criteria each parcel meets. The six binary criteria are: (1) within 2km of an electrical substation, (2) larger than 40 hectares, (3) currently under low-value land use (fallow/idle cropland, grassland/pasture, developed land, or barren/shrubland), (4) in the top quartile of drought exposure, (5) above the 25th percentile of solar irradiance, and (6) in the bottom quartile of soil quality. Parcels scoring 5 or 6 represent high-priority sites combining strong solar potential with limited agricultural value. Parcels under low/medium/high developed land use are set to zero.

Figure A6: Comparison of Simple and Continuous Solar Suitability Measures

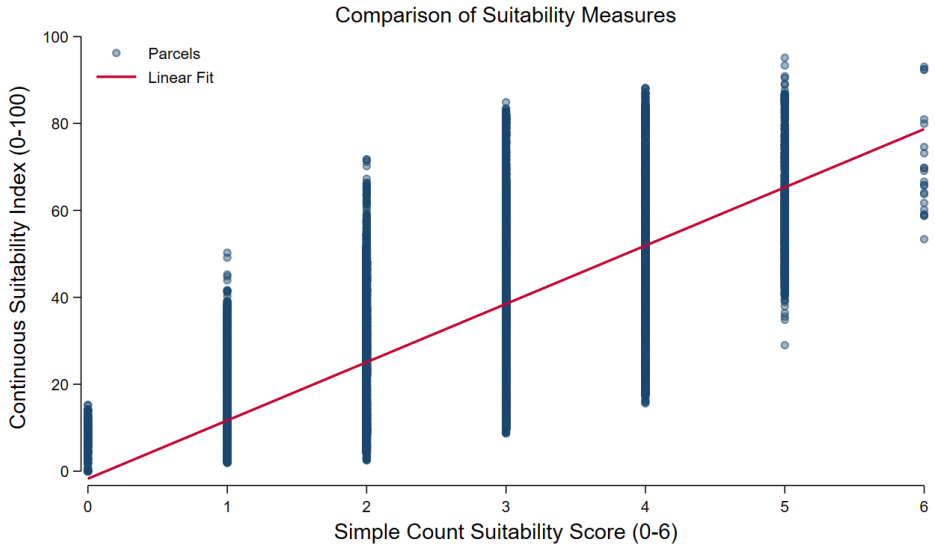

Note: Scatter plot comparing the simple count suitability index (0-6) with the continuous weighted suitability index (0-100) for parcels with no solar installations as of 2023. The simple index counts binary criteria (within 2km of substation, larger than 40ha, low-value land use, top quartile drought, above-median solar irradiance, bottom quartile soil quality). The continuous index applies linear penalty functions to the same underlying characteristics and weights them by standardized regression coefficients.

Figure A7: High-Priority Sites for Solar Development

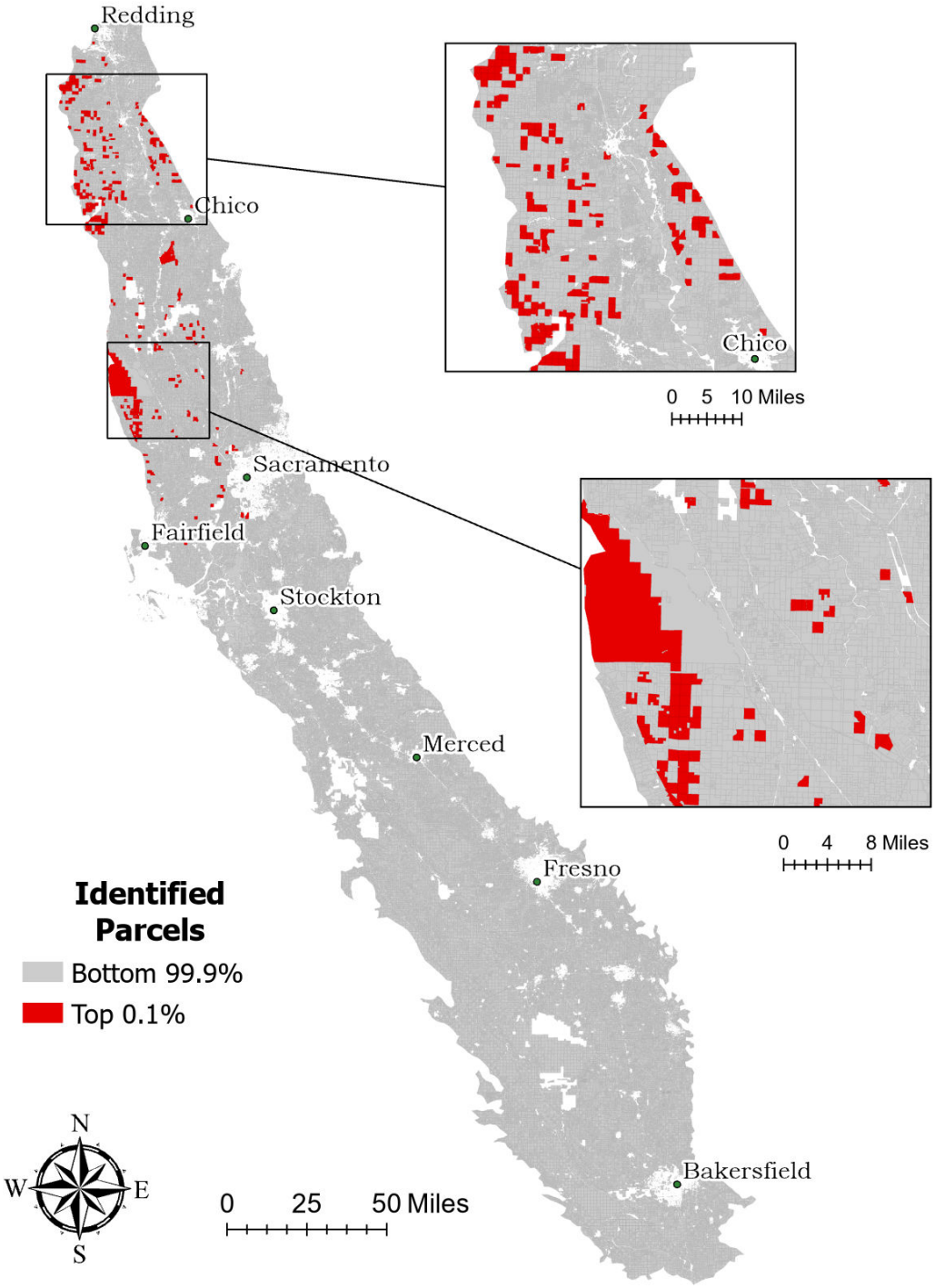

Note: Map shows 328 parcels scoring at or above the 99.9th percentile of the continuous solar suitability index among parcels that did not have solar installations as of 2023. These high-priority sites combine strong technical suitability for solar development (proximity to electrical infrastructure, large parcel size, high solar irradiance) with low agricultural value (high drought exposure, poor soil quality, low-value land uses). Parcels under low/medium/high developed land use are excluded.

Figure A8: Predicted Probability of Post-2018 Solar Adoption by 2018 Suitability Decile

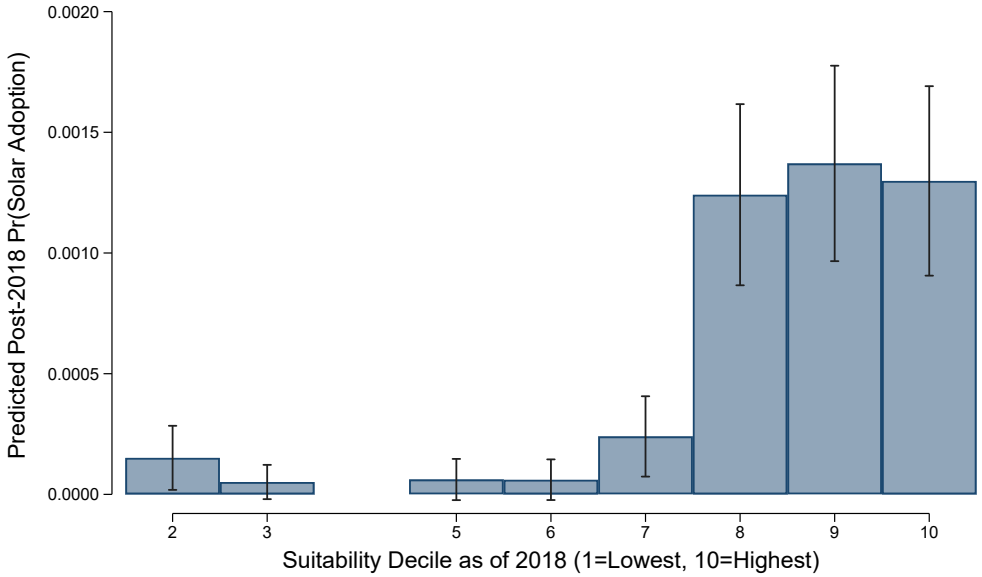

Note: Figure plots marginal effects from a logistic regression of post-2018 solar adoption on 2018 suitability deciles. The model uses suitability scores constructed from 2006-2018 data and applied to 2018 parcel characteristics.

Figure A9: ROC Curve for Suitability Index Prediction

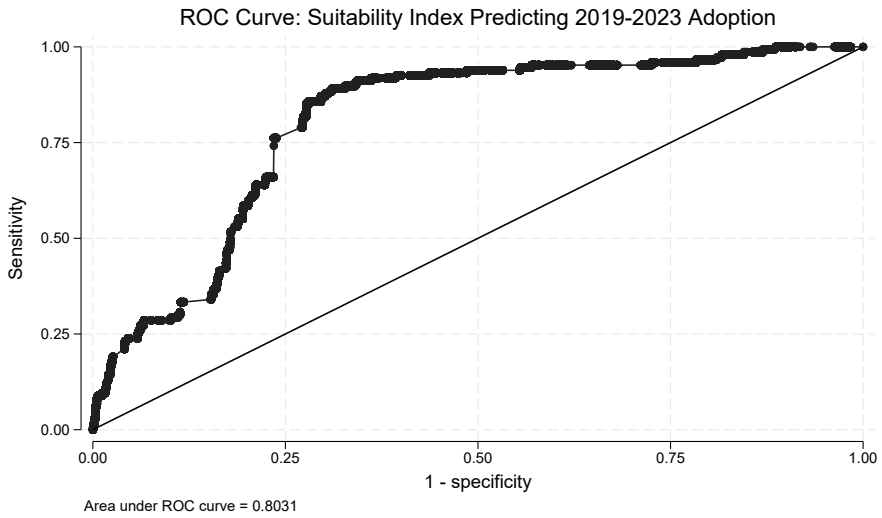

Note: Receiver operating characteristic (ROC) curve showing the predictive performance of the suitability index for 2019-2023 solar adoption. The index is constructed using coefficients estimated on 2006-2018 data and applied to 2018 parcel characteristics.

Table A7: Robustness: 1-Year Lagged Drought and Labor Costs

	Solar Adoption (0/1)		
	(1)	(2)	(3)
Drought Exposure (t-1)	0.0007***	-0.0050*	-0.0150***
	(0.0002)	(0.0026)	(0.0023)
Labor Cost (log, t-1)	0.0013***	0.0013***	0.0014***
	(0.0002)	(0.0001)	(0.0001)
Poor Soil Quality	0.0010***	0.0007***	
	(0.0002)	(0.0001)	
Solar Irradiance	0.0084***	0.0054***	
	(0.0007)	(0.0005)	
Proximity to Substation	0.0009***	0.0006***	
	(0.0001)	(0.0001)	
Proximity to T-Lines	0.0002***	0.0001	
	(0.0001)	(0.0000)	
Parcel Area (log)	0.0003***	0.0002***	
	(0.0000)	(0.0000)	
Interactions			
Drought × Labor Cost		-0.0004	0.0009***
		(0.0004)	(0.0003)
Drought × Poor Soil Quality		0.0007***	0.0005***
		(0.0002)	(0.0001)
Drought × Solar Irradiance		0.0066***	0.0075***
		(0.0007)	(0.0007)
Drought × Proximity Substation		0.0007***	0.0006***
		(0.0001)	(0.0001)
Drought × Proximity T-Lines		0.0003***	0.0002***
		(0.0001)	(0.0001)
Drought × Parcel Area (log)		0.0003***	0.0002***
		(0.0000)	(0.0000)
Year Fixed Effects	Yes	Yes	Yes
Parcel Fixed Effects	No	No	Yes
Observations	2,996,298	2,996,298	2,996,298
Adjusted R-squared	0.00190	0.00202	0.00122

Notes: Table reports linear probability model estimates with robust standard errors clustered at the parcel level in parentheses. Drought and labor cost exposure are measured with a 1-year lag, rather than the 3-year lag used in the preferred specification. Model (1) includes main effects only. Model (2) adds interactions between drought exposure and parcel characteristics. Model (3) includes parcel fixed effects. Distance to transmission lines is included as a control but not shown for brevity (coefficient ≈ 0).
*** $p < 0.01$, ** $p < 0.05$, * $p < 0.1$.

Table A8: Robustness: 5-Year Lagged Drought and Labor Costs

	Solar Adoption (0/1)		
	(1)	(2)	(3)
Drought Exposure (t-1 to t-5)	0.0082***	-0.0717***	-0.0819***
	(0.0008)	(0.0085)	(0.0070)
Labor Cost (log, t-1 to t-5)	0.0022***	-0.0007***	0.0006***
	(0.0002)	(0.0002)	(0.0002)
Poor Soil Quality	0.0011***	-0.0002*	
	(0.0002)	(0.0001)	
Solar Irradiance	0.0056***	-0.0015***	
	(0.0005)	(0.0006)	
Proximity to Substation	0.0009***	-0.0005***	
	(0.0001)	(0.0001)	
Proximity to T-Lines	0.0002***	0.0000	
	(0.0001)	(0.0000)	
Parcel Area (log)	0.0003***	-0.0001***	
	(0.0000)	(0.0000)	
Interactions			
Drought × Labor Cost		0.0092***	0.0092***
		(0.0012)	(0.0009)
Drought × Poor Soil Quality		0.0033***	0.0023***
		(0.0006)	(0.0005)
Drought × Solar Irradiance		0.0195***	0.0228***
		(0.0024)	(0.0024)
Drought × Proximity Substation		0.0036***	0.0029***
		(0.0005)	(0.0004)
Drought × Proximity T-Lines		0.0004*	0.0001
		(0.0002)	(0.0002)
Drought × Parcel Area (log)		0.0010***	0.0008***
		(0.0001)	(0.0001)
Year Fixed Effects	Yes	Yes	Yes
Parcel Fixed Effects	No	No	Yes
Observations	3,028,229	3,028,229	3,028,229
Adjusted R-squared	0.00207	0.00256	0.00172

Notes: Table reports linear probability model estimates with robust standard errors clustered at the parcel level in parentheses. Drought and labor cost exposure are measured with a 5-year lag, rather than the 3-year lag used in the preferred specification. Model (1) includes main effects only. Model (2) adds interactions between drought exposure and parcel characteristics. Model (3) includes parcel fixed effects. Distance to transmission lines is included as a control but not shown for brevity (coefficient ≈ 0).
*** $p < 0.01$, ** $p < 0.05$, * $p < 0.1$.

Table A9: Robustness: Omitting Soil Quality

	Solar Adoption (0/1)		
	(1)	(2)	(3)
Drought Exposure (t-1 to t-3)	0.0022***	-0.0031	-0.0222***
	(0.0004)	(0.0030)	(0.0024)
Labor Cost (log, t-1 to t-3)	0.0013***	0.0012***	0.0019***
	(0.0002)	(0.0001)	(0.0002)
Solar Irradiance	0.0057***	0.0031***	
	(0.0005)	(0.0003)	
Proximity to Substation	0.0009***	0.0002***	
	(0.0001)	(0.0000)	
Proximity to T-Lines	0.0002***	0.0001***	
	(0.0001)	(0.0000)	
Parcel Area (log)	0.0003***	0.0001***	
	(0.0000)	(0.0000)	
Interactions			
Drought × Labor Cost		-0.0005	0.0018***
		(0.0005)	(0.0003)
Drought × Solar Irradiance		0.0062***	0.0086***
		(0.0008)	(0.0008)
Drought × Proximity Substation		0.0016***	0.0013***
		(0.0002)	(0.0002)
Drought × Proximity T-Lines		0.0002	0.0000
		(0.0001)	(0.0001)
Drought × Parcel Area (log)		0.0004***	0.0003***
		(0.0000)	(0.0000)
Year Fixed Effects	Yes	Yes	Yes
Parcel Fixed Effects	No	No	Yes
Observations	3,453,496	3,453,496	3,453,496
Adjusted R-squared	0.00178	0.00197	0.00130

Notes: Table repots linear probability model estimates with robust standard errors clustered at the parcel level in parentheses. This specification omits poor soil quality, which is unavailable for some Central Valley areas, resulting in the exclusion of 27 solar facilities from the sample. Model (1) includes main effects only. Model (2) adds interactions between drought exposure and parcel characteristics. Model (3) includes parcel fixed effects.
*** $p < 0.01$, ** $p < 0.05$, * $p < 0.1$.

Table A10: Logit Marginal Effects: Solar Adoption

	Solar Adoption (0/1)	
	(1)	**(2)**
Drought Exposure (t-1 to t-3)	0.0007**	0.0008**
	(0.0003)	(0.0003)
Labor Cost (log, t-1 to t-3)	0.0040***	0.0039***
	(0.0005)	(0.0005)
Poor Soil Quality	0.0009***	0.0009***
	(0.0002)	(0.0002)
Solar Irradiance	0.0288***	0.0286***
	(0.0028)	(0.0028)
Proximity to Substation	0.0008***	0.0008***
	(0.0001)	(0.0001)
Proximity to T-Lines	0.0002***	0.0002***
	(0.0001)	(0.0001)
Parcel Area (log)	0.0004***	0.0004***
	(0.0000)	(0.0000)
Year Fixed Effects	Yes	Yes
Observations	2848684	2848684

Notes: Table reports average marginal effects from logit models with robust standard errors clustered at the parcel level in parentheses. Marginal effects represent the change in adoption probability (in percentage points) for a one-unit change in each variable, evaluated at sample means. Model (1) includes main effects only. Model (2) adds interactions between drought exposure and parcel characteristics.
*** $p < 0.01$, ** $p < 0.05$, * $p < 0.1$.

Table A11: Logit Marginal Effects: Impact of Prior Land Use on Solar Adoption

	Solar Adoption (0/1)
Drought Exposure (t-1 to t-3)	0.0005*
	(0.0003)
Labor Cost (log, t-1 to t-3)	0.0029***
	(0.0005)
Poor Soil Quality	0.0006***
	(0.0002)
Solar Irradiance	0.0227***
	(0.0025)
Proximity to Substation	0.0007***
	(0.0001)
Proximity to T-Lines	0.0002***
	(0.0001)
Parcel Area (log)	0.0004***
	(0.0000)
Land Use (t-1)	
Cereal Grains	0.0005***
	(0.0001)
Feed, Fiber, Industrial Crops	-0.0002*
	(0.0001)
Fruits	-0.0002**
	(0.0001)
Vegetables and Melons	0.0000
	(0.0002)
Nuts	-0.0002***
	(0.0001)
Tree Crops	0.0009
	(0.0006)
Fallow/Idle Cropland	0.0017***
	(0.0002)
cdl_type_t1=9	0.0013
	(0.0016)
Developed Land	0.0020***
	(0.0004)
cdl_type_t1=11	-0.0003***
	(0.0001)
Forest/Wetlands	-0.0003
	(0.0002)
Year Fixed Effects	Yes
Observations	2848684

Notes: Table reports average marginal effects from logit model with robust standard errors clustered at the parcel level in parentheses. Land use categories are measured in year t-1 (prior to potential solar adoption). Reference category: Grassland/Pasture. Water parcels are excluded from the analysis.
*** $p < 0.01$, ** $p < 0.05$, * $p < 0.1$.

Figure A10: Effect of Prior Land Use on Solar Adoption (Logit)

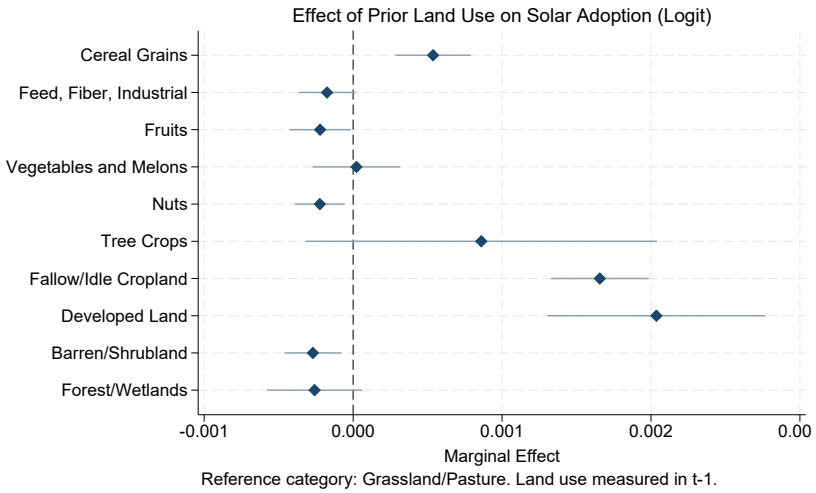

Notes: Coefficient plot from logit model showing the effect of prior land use (t-1) on solar adoption probability. Points represent marginal effects with 95% confidence intervals. Reference category: Grassland/Pasture. Water parcels excluded from analysis. Robust standard errors clustered at the parcel level.